ELUCIDATING CRITICAL FACTORS FOR PRACTICAL DRY CLEANING APPLICATIONS ON LOW-MOISTURE FOOD CONTACT SURFACES

By

Ian Michael Klug

A THESIS

Submitted to
Michigan State University
in partial fulfillment of the requirements
for the degree of

Biosystems Engineering – Master of Science

2023

ABSTRACT

Recent outbreaks linked to flour-based products have highlighted the need for improved cleaning and sanitation methods in low-moisture environments. The factors affecting adhesion forces of flour particles, and the effective vacuum cleaning methodologies to overcome these forces, need to be better understood. The objectives of this study were to: (1) Measure electrostatic charge build-up in flour under different environmental conditions (20, 40, 60% relative humidity at room temperature), (2) quantify how powder size (US standard No. 60 – 80 or 80 – 100 mesh), electrostatic charge (charged and uncharged), and relative humidity (RH) impact the force required to remove the powder from an electropolished 304 stainless steel coupon (8 × 8 × 0.2 cm), and (3) determine the most effective vacuum nozzle angle (0, 45, 90° relative to the surface) for cleaning. Chargeability (nC) of flour samples was assessed using a Faraday cup electrometry, while the surface adhesion force of the flour particles was measured using a custom-built impact tester. Additionally, the surface cleanliness after vacuum treatments was assessed using ATP (adenosine triphosphate) swabs and a luminometer. Charged flour samples at 20% RH exhibited a significantly higher charge compared to those at 40 and 60% RH. Within the 60 – 80 mesh range, charged flour showed higher adhesion rates than uncharged samples at both 20% and 40% RH. However, in the 80 – 100 mesh range, charged flour did not show a significant difference in adhesion when compared to uncharged samples at any relative humidity level. Additionally, at 60% RH, surface residues measured by ATP were significantly lower for vacuum angle 90° than for 0° across both 60 – 80 mesh and 80 – 100 mesh size ranges of wheat flours.

ACKNOWLEDGEMENTS

First and foremost, I would like to sincerely thank my major advisor Dr. Sanghyup Jeong for his guidance and support. His unique style of problem solving taught me that oftentimes you need to approach an issue from many angles before finding the correct path forward. When I experienced setbacks within my experimental design, he reassured me that starting from scratch does not equate to failure. Without his patience and encouragement, this work would not have been possible.

I am also appreciative of my committee members Dr. Bradley Marks and Dr. Teresa Bergholz for their confidence in my research. Even when time was limited, they prioritized reviewing my work and providing thoughtful feedback. A special thanks is extended to lab managers Michael James and Ian Hildebrandt. They ensured that the lab space, equipment and help I needed to succeed was always available. Their outside perspectives and wealth of prior knowledge and experience were instrumental to my success.

I am grateful to the BAE fabrication shop specialist Philip Hill, whose mechanical expertise I could rely on to help construct and iterate upon the novel equipment used in this experiment. Thank you to fellow grad student Kase Nelson, who helped me brush, swab, swab some more, and reminded me to eat and sleep.

Finally, thank you to my mother and father, for their love and encouragement, and my sister for keeping my spirits high. Knowing that I always had your unwavering support and a home to come back to gave me the confidence I needed to succeed.

This work is supported by the Agriculture and Food Research Initiative, Sustainable Agricultural Systems Program grant no. 2020-68012-31822 from the USDA National Institute of Food and Agriculture. Any opinions, findings, conclusions, or recommendations expressed in

this publication are those of the author(s) and do not necessarily reflect the view of the U.S. Department of Agriculture

TABLE OF CONTENTS

INTRODUCTION

Problem Statement

Recently, raw flour has emerged as a potential health hazard, with several *E. coli* and *Salmonella* outbreaks linked to flour and flour-based products in the past five years (United States Food and Drug Administration, 2019; Centers for Disease Control and Prevention, 2021; United States Food and Drug Administration, 2023). Research shows that pathogens can survive and express virulence in raw flour for extended periods, even years (Forghani et al., 2019; Gill et al., 2020; Lauer et al., 2021). Consequently, investigating methods to reduce flour contamination is crucial for public health safety.

In addressing this challenge, one key aspect to consider is that pathogens in flour products often stem from cross-contamination from equipment surfaces. Therefore, implementing effective cleaning and sanitation practices becomes vital in preventing this transfer. This process begins with the removal of food debris from surfaces, an essential step to ensure successful sanitation. For cleaning to be effective, it must counteract the adhesion forces binding food debris to surfaces. Especially, in low-moisture environments like flour processing, electrostatic adhesion is often predominant. This occurs through triboelectrification, where flour particles gain electrostatic charge from friction against equipment surfaces.

Notably, in low-moisture food processing industry, vacuuming is widely adopted method for cleaning. The increased adhesion from electrostatic forces and its effect on vacuum cleaning efficacy needs further investigation. Hence, a deeper understanding of the cleaning technique and the role of environmental conditions is imperative to maximize the effectiveness of vacuum cleaning and ultimately enhance food safety.

Goals and Objectives

Previous studies have attempted to measure the adhesive force of flour particles, evaluating the impact of factors such as particle size, relative humidity, and electrostatic charge. Nonetheless, these methodologies and factors have not been investigated regarding cleaning food contact surfaces in low-moisture food environments. The triboelectrification of flour during processing on stainless steel and the efficacy of conventional cleaning methods on overcoming the adhesive forces, remain unexplored. My research aimed to address this gap in knowledge. Therefore, the goal of the study was to investigate the factors that affect flour adhesion to a food contact surface and to suggest optimal cleaning methods. The specific objectives of my research were to:

1. Measure electrostatic charge build-up in flour under different environmental conditions.
2. Quantify how powder size, electrostatic charge, and relative humidity impact the force required to remove the powder from a stainless steel surface.
3. Determine the most effective angle for vacuum cleaning for enhanced surface cleanliness under different environmental conditions.

LITERATURE REVIEW

Flour as a Product of Concern

Recent outbreaks associated with raw flour and flour-based products have highlighted flour as a potential public health concern. The first outbreak linked to flour occurred in 2016, with *Escheria coli* in raw flour. This outbreak resulted in 56 cases of infection spread over 24 states and could be traced back to a single domestic flour production facility (Crowe et al., 2017). More recently, over the past few years, there have been alarming instances of food contamination, starting with the recall of Brand Castle and Sisters Gourmet cookie and brownie mixes on June 21st, 2018, due to possible *Escherichia coli* contamination (United States Food and Drug Administration, 2019). The situation took another concerning turn on September 16th, 2021, when a multistate outbreak of Shiga toxin-producing *Escherichia coli* (STEC) was traced back to cake mix (Centers for Disease Control and Prevention, 2021). Adding to the series of outbreaks, on March 30th, 2023, the US Food and Drug Administration announced an outbreak of *Salmonella* linked to all-purpose flour (United States Food and Drug Administration, 2023) which highlights the continued challenges in ensuring food safety.

From 2012 – 2020, food in the cereal, bakery, and grain category was responsible for 14.8% of low-moisture food outbreaks, but only 6% of recalls (Acuff et al., 2023). This discrepancy can be attributed to the recent growing awareness of flour as a food of concern. A 3-year investigation on the prevalence of pathogens on 3891 wheat berries samples found that enterohemorrhagic *E. coli* and *Salmonella* could be found on 0.44% and 1.23% of tested wheat berries respectively (Myoda et al., 2019). Despite the inhibitory effect of low water activity in low-moisture foods, which typically hinders microbial growth, pathogens may survive for years on wheat grains and flour while maintaining their ability to express virulence factors (Forghani et

al., 2019; Gill et al., 2020; Lauer et al., 2021). All these recent outbreaks and findings clearly implicate flour as a low-moisture food of concern.

Cross-contamination in Low-Moisture Environments

The Food Safety Modernization Act (FSMA), enacted in 2011 to transform the approach to food safety from reactive to proactive, aims to prevent contamination by establishing preventative controls for all types of food, including low-moisture products. While FSMA requires a validated kill step for pathogens in dry environments on the food itself, it does not provide specific guidelines for processing equipment. Thus, cleaning and sanitation procedures largely remain at the manufacturer's discretion. Cleaning is the process of removing food residues or allergens from equipment surfaces, while sanitation focuses on inactivating bacteria and pathogens. While conventional dry-cleaning methods may achieve some minimal bacterial reduction (Chen & Snyder, 2023), a subsequent sanitation step is often required. Cleaning is crucial to prevent cross contamination and to prepare surfaces for sanitization.

Surface cross-contamination generally occurs when pathogens are transferred from one surface or object to another. Food products that come in contact with contaminated equipment surfaces during processing may become carriers of pathogenic bacteria. If cross-contamination to food occurs after pathogenic inactivation steps, it can pose a significant health risk to consumers. In the case of an outbreak, potentially all product on the market may need to be recalled unless a clean break was established. A World Health Organization survey determined cross-contamination was responsible for a significant proportion of foodborne outbreaks in Europe (World Health, 1995). The report indicated that cross-contamination accounted for 3.6% of cases of pathogens in prepared foods, while contaminated equipment was implicated in 5.7% of cases. Additionally, Powell & Attwell (1998) compile several outbreaks occurring in the United

Kingdom. For outbreaks where the contributing factor was known, 57% of cases could be attributed to cross-contamination. A review article by Podolak et al. (2010) demonstrated that cross-contamination could occur in a variety of low-moisture foods despite the hurdle to bacterial growth provided by low water activity. This demonstrates the importance of cleaning equipment surfaces to reduce the risk of cross-contamination.

Cleaning Methods in Low-Moisture Environments

Flour, a low-moisture food with water activity below 0.85, illustrates the challenges in cleaning and sanitizing such environments where limiting water introduction is crucial to prevent bacterial growth. Consequently, cleaning methods for low-moisture settings are generally limited to brushing, vacuum cleaning, scraping, sweeping, blowing/blasting, or pigging due to this constraint (Moerman & Mager, 2016).

Each cleaning method for low-moisture environments has its own advantages and drawbacks. For optimal effectiveness, employing combination of various tools is recommended. Vacuum cleaning is often the initial step in dry cleaning open process equipment (Moerman & Mager, 2016). An advantage of vacuum cleaning is its ability to contain soil without needing a secondary collection step. Vacuums reduce the dispersal of dust and particles to other areas of the food plant, and their smaller, mobile units can be easily moved through the facility. While vacuums effectively remove visible particles, they are less effective for thorough cleaning and may struggle to remove particles that are strongly adhered (Moerman & Mager, 2016). Following a vacuum treatment, brushing or scraping can be applied for a more in-depth clean and to remove the strongly adhered particles. However, if not used properly, brushing may generate clouds of debris that can spread and contaminate other areas.

Figure 1: Transportable vacuum unit used to clean pilot scale food production equipment

Recent studies have focused on brushing and scraping food residue in low-moisture environments. In a 2022 study, Chen et al. (2022), developed a custom platform to apply brushing and scraping treatments to soiled food contact surfaces mechanically and consistently. The findings indicated that brushing was more effective than scraping for removal of powder from surfaces. However, food residues could still be detected at higher water activity levels after brushing. Additionally, the study found that under the tested conditions, surface roughness did not significantly impact the efficacy of cleaning. Later experiments performed by Quanrun et al. (2022), used the same mechanical brush system to evaluate how residence time of fruit powders impacted ease of removal. This study found that longer residence times resulted in higher water activities for most powders, and that most fruit powders with a higher water activity exhibited higher cohesion and adhesion.

A survey revealed that 24 to 64% of food manufacturing facilities utilize vacuums as a dry-cleaning tool (Taylor et al., 2006). Despite its importance and widespread use in the dry-

cleaning process, research on vacuum cleaning within the food production environment remain scarce. The optimal placement for a vacuum nozzle is about 1 – 2 cm above the surface to maximize suction flow (Moerman & Mager, 2016). This distance is often maintained through nozzle attachments, such as brushes. A study performed by Jackson, et al. (2008), examined the efficiency of vacuum cleaners in removing food residues from several food contact surfaces: stainless steel, Teflon, and polyurethane. The study found that while vacuuming could remove loosely adhered foods to a level of visually clean for most surfaces, assays like ELISA, protein swabs, and ATP swabs could still detect residues after vacuuming, suggesting that vacuuming alone is not sufficient for removing allergenic food residues. However, the study did not address how factors such as particle size, electrostatic charge, relative humidity, and angle of the vacuum nozzle might impact the effectiveness of vacuuming.

Methods of Quantifying Cleanliness

To validate the efficacy of a cleaning treatment, it is important to have a method to quantify cleanliness on equipment surfaces. Surface cleanliness measurement methods can be categorized as direct or indirect, and specific or nonspecific. For direct methods of surface analysis, equipment surfaces are directly monitored for contamination. Common examples of direct quantification utilize magnified visual inspection, scanning or transmission electron microscope, and x-ray detectors (Kohli & Mittal, 2019). Direct methods can be time-consuming and are typically limited to examining a small representative surface area. Because of these limitations, indirect surface sampling is often preferred. Indirect methods extract the contaminant from the surface, usually through swabbing, and then analyze the extract for the contaminant. Specific methods can identify and differentiate between strains of bacteria or allergenic proteins. Pathogens and allergens often have specific and well-defined detection methods and are

preferred by regulatory authorities. However, general surface debris like dust, soil, and non-allergenic food residues mostly rely on nonspecific detection methods.

One of the most common and simplest methods of direct, nonspecific cleanliness measurement is visual examination, which is qualitative and depends on the cleaner's best judgement. Cleaners are often instructed to clean equipment surfaces until they appear "visibly clean" of any debris or residue. A recent study (Daeschel et al., 2023) investigated the limits of visual detection on equipment surfaces. Surface of stainless steel and high-density polyethylene were either left clean or soiled with dry wheat flour. When 101 respondents visually inspected these surfaces for food residues, about half of the respondents failed to detect as little as 0.02 g of flour per square foot (929 cm^2) on stainless steel. This finding suggests the need for additional cleanliness verification methods beyond human visual detection. Swabbing for ATP is a more rigorous method of measuring cleanliness.

ATP swabbing is an indirect, nonspecific, and quantitative method for measuring cleanliness in low-moisture food production environments. ATP, or Adenosine triphosphate, is an organic compound present in all living things: bacteria, plants, and animals. ATP can be extracted from equipment surfaces using typical swabbing techniques. First, a solvent with the ability to extract the contaminant is used to moisten the swab. Next, the surface of interest is swabbed vertically and horizontally for a predetermined number of strokes, while ensuring to coat all sides of the swab (Kohli & Mittal, 2019). Following swabbing, the ATP coated swab is introduced to an enzyme that reacts with ATP to generate light. The amount of light generated by the reaction is stronger the more ATP is present. The amount of light can be measured in Relative Light Units (RLU) by a luminometer to quantify surface cleanliness. In food processing plants, it is typically recommended for food processors to swab adequately cleaned surfaces to

obtain a specific RLU value that signifies “clean” surfaces. This value is then established as a predetermined cut-off for clean surfaces in future assessments.

A drawback of using ATP as a method for quantifying cleanliness is that it cannot differentiate between ATP from food residues, harmless bacteria, human hands, or pathogens. Despite its lack of specificity, ATP swabbing has been an appealing rapid method to analyze equipment surfaces for contaminants due to its speed (< 30 seconds) when compared to other methods. Historically, ATP has successfully been used to rapidly monitor microbial populations on food contact surfaces (Hammons et al., 2015; Sogin et al., 2021). However, this methodology could be applied to food residue detection after a cleaning step if the only source of ATP on a surface is the from the food itself or background microbes on the food. It is desirable for more research to be conducted on ATP swabbing as a method of detecting food residues after a cleaning step, especially within low-moisture food production environments.

Forces of Adhesion

To be effective, vacuum cleaning force must overcome the adhesion forces between particles and surfaces. These forces include Van der Waals, capillary, and electrostatic forces (Ermis et al., 2011). However, in low-moisture environments, electrostatic force and Van der Waals forces are predominant (Huang & Barringer, 2012).

Van der Waals forces result from the interactions between dipoles of atoms and molecules. Areas of molecules with an electron abundance have a partial negative charge and are attracted to areas of molecules deficient of electrons that are partially positive. Van der Waals forces are secondary forces and are less dependent on the chemical structure of materials and weaker when compared to primary forces such as covalent or ionic. However, Van der Waals forces can have a greater reach than primary forces. In the absence of chemical bonds and

external electrical fields, the primary force of adhesion between dry powder particles and other surfaces are typically Van der Waals (Salazar-Banda et al., 2007).

As food powders are processed on-line, the friction and contact of food particles against each other and the stainless steel processing equipment causes a buildup of electrostatic charge through a process known as triboelectrification (Bailey, 1984; Chowdhury et al., 2021). Particles with a negative charge will be attracted to surfaces with a positive charge and vice-versa. For surfaces that are not electrically charged, the conductivity of the surface plays an important role. For conductive materials, like stainless steel, when a charged particle approaches, a charge of the equal and opposite polarity will be drawn out from the side of the conductor closest to the particle. This phenomenon is known as electrostatic induction. Grounding the conductor does not stop the process of electrostatic induction, however it can prevent larger opposite charges from building up within the conductor.

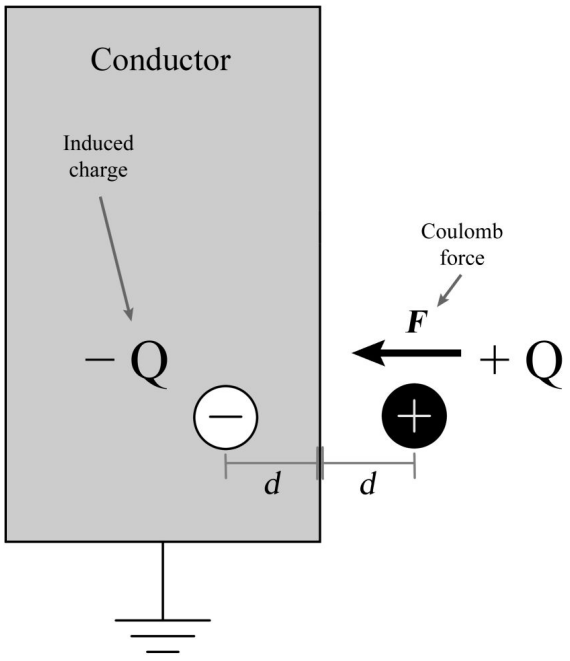

Figure 2: Electrostatic induction of a grounded conductor by a charged particle

Environmental relative humidity greatly affects particle chargeability. At a given temperature, higher relative humidity levels lead to reduced charge accumulation and retention on particles (Matsusaka et al., 2010). Ideally, processing of low-moisture foods should occur in a low relative humidity environment; however, controlling ambient humidity can be difficult. Additionally, the size of the particle significantly influences its adhesion force, with larger particles potentially having stronger electrostatic attraction to equipment surfaces because they can carry more charge.

Measuring Adhesion

Measuring the adhesion force between a particle and a surface in practice can be challenging. Atomic force microscopy (AFM) and the centrifuge technique are the two most commonly accepted methods (Salazar-Banda et al., 2007). However, new methods have been developed that offer advantages under the right circumstances. For example, the impact adhesion tester (IAT) measures adhesion with principles similar to the centrifuge technique but offers a quicker and more compact alternative (Ermis et al., 2011).

The atomic force microscope can generate three-dimensional mappings of surfaces by dragging the tip of a precise cantilever (<1 nm thick tip) across the surface of interest. This instrument can be adapted for broader adhesion force measurements between particles and the surface of interest. This is done by affixing the particle of interest to the tip of the cantilever and manipulating the distance of the device from the surface (Suehr, 2020). As the cantilever is retracted from the test surface, the deflection of the cantilever is used to quantify the adhesion force between particle and surface. The precision of measurements provided by this technique make it one of the most common methods for quantifying particle adhesion. Nevertheless, this technique has limitations when trying to measure the adhesion of particles of variable sizes on a

surface. This technique can only measure the removal force for one particle at a time, meaning powders with a variable range of particle sizes are difficult and time consuming to characterize (Salazar-Banda et al., 2007).

The centrifuge technique can provide a more effective measure of particle adhesion for particles with varied shapes and sizes. This technique applies centrifugal forces to particles adhered to a surface (Salazar-Banda et al., 2007). It is assumed that the force of adhesion between a particle and a surface has an equal but opposite magnitude to the centrifugal force required to remove the particle. For this method to be effective, the surface the particles are adhered upon must be rotated in a way such that the centrifugal forces are acting normally on the particles from the surface. Following centrifugal treatment, either imaging or mass measurements can be used to determine the percentage of particles removed by the treatment (Salazar-Banda et al., 2007). By applying several different rotational speeds, the relationship between applied force and percentage of particles removed can be characterized. A common method of applying the rotational force to particles is through a centrifuge, common to most microbiology labs (Suehr, 2020). The coated surface of interest can be placed within a centrifuge tube and angled so that force is applied normally to the surface (Ermis et al., 2011; Suehr, 2020; You & Wan, 2014). Although more practical than AFM for assessing adhesion of powders, the centrifuge method requires sizable, costly equipment, making it less suitable for space constrained studies.

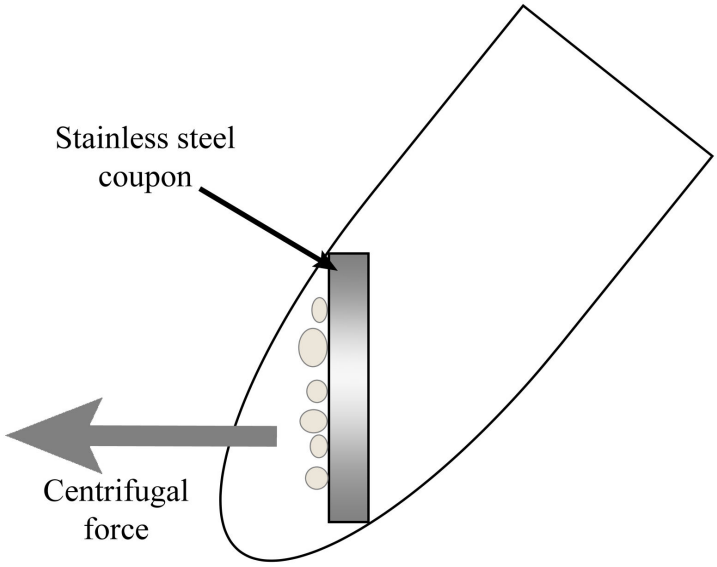

Figure 3: Centrifuge method of measuring particle adhesion

Previous research has compared the efficacy of the centrifuge method of measuring adhesion with the drop test (Stotzel et al., 1997), finding similar outcomes despite differing force application techniques. Ermis et al. (2011) designed a compact, portable impact adhesion tester suitable for inline production assessment. The IAT, operating on similar principles to the centrifugal technique, applies impact rather than centrifugal forces to dislodge particles. The IAT has a platform that can move freely along a vertical cylindrical shaft, which, when elevated and released, impacts the sample coated underneath, dislodging particles perpendicularly. The percentage of particles removed can be measured through mass or through microscopic imaging and counting of particles. The impact force varied proportionately with the height the platform was dropped from. By applying several different impact forces, the relationship between applied force and percentage of particles removed can be characterized.

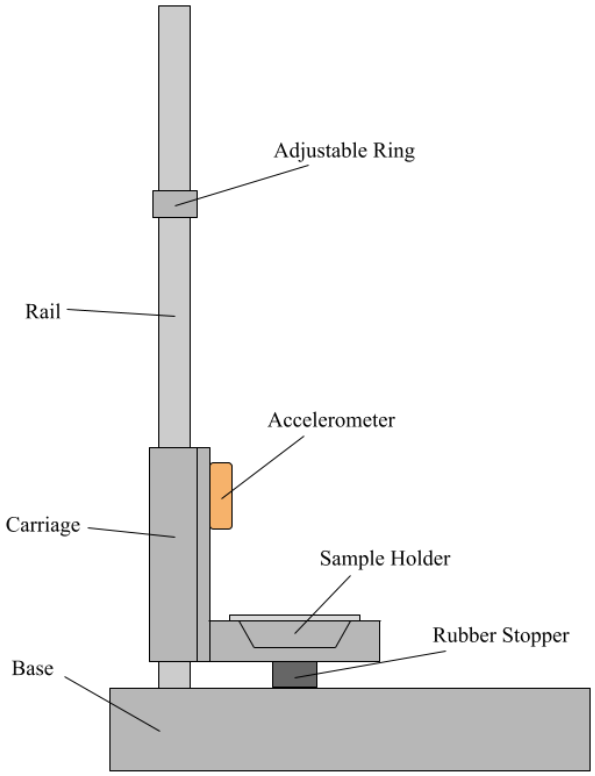

Figure 4: Labeled diagram of an impact adhesion tester

The previously mentioned methods of quantifying adhesion were designed to measure the adhesion of individual particles on a surface. However, bulk powders and their inter-particle interactions exhibit distinct behaviors. To evaluate the adhesion and cohesion of bulk powders, Chen et al., (2022) utilized a force gauge to measure the necessary shear force for characterizing adhesion of powdered food residues on stainless steel surfaces. For this, two stainless steel rings of the same diameter were fabricated, one completely open and the other with a bottom. For adhesion tests, the open ring was placed in the center of a stainless steel coupon and filled with a known mass of powder to ensure consistent bulk density in contact with the stainless steel coupon. Then a digital force gauge was used to slide the open ring across the coupon surface while measuring the necessary shear force. In cohesion tests, the open ring was placed over the closed ring and then filled with a known mass of powder. Again, the digital force gauge was

used to apply and measure the shear force needed to slide the open ring over the stationary closed ring. Control tests with empty rings determined the inherent force to displace the rings, which was subtracted from final readings. While this approach effectively measures bulk powder shear force, it may not represent real-world cleaning situations involving finely dispersed powders over a surface.

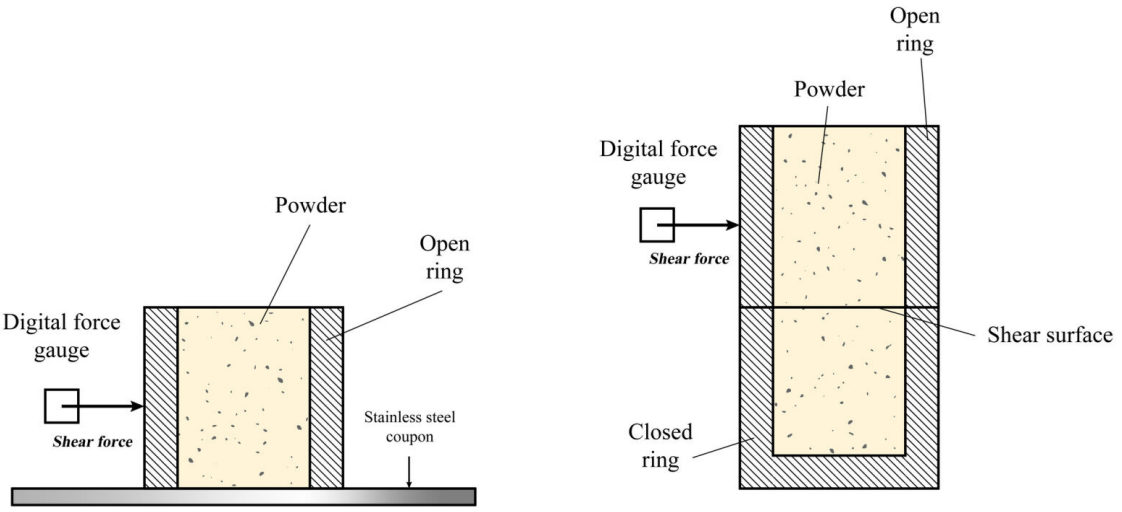

Figure 5: Shear force experiments for adhesion and cohesion of particles on a stainless steel surface. Adapted from Chen et al. (2022)

Measuring Electrostatic Charge

Several instruments are available to determine the electrostatic charge of objects. The electrostatic fieldmeter is one such instrument, which quantifies the electrostatic field produced by charged surfaces at a known distance, measuring charge as voltage over distance (Peltonen, 2019). Measurements are taken using a high input impedance sensor referenced to the ground. While this tool can be useful in detecting charge generation, it can be difficult to use for precise charge measurements. The area of the surface being measured compared to the sensors field of

view, distance from the sensor to the surface, and proximity of other charged objects can all potentially skew the measurements.

A more common and precise tool for measuring charge of powders is a Faraday cup and electrometer. A Faraday cup consists of two concentric aluminum cups separated by an insulator. The outer cup is grounded and shields the inner from external electric fields. When a charged object enters the inner cup, it induces an equal but opposite charge on the inner wall (Peltonen, 2019). The electrometer then measures the charge difference in charge between inner and outer wall. By measuring the mass of the powder sample subsequently, the charge-to-mass ratio of a sample can be obtained for comparison between treatments (Peltonen, 2019).

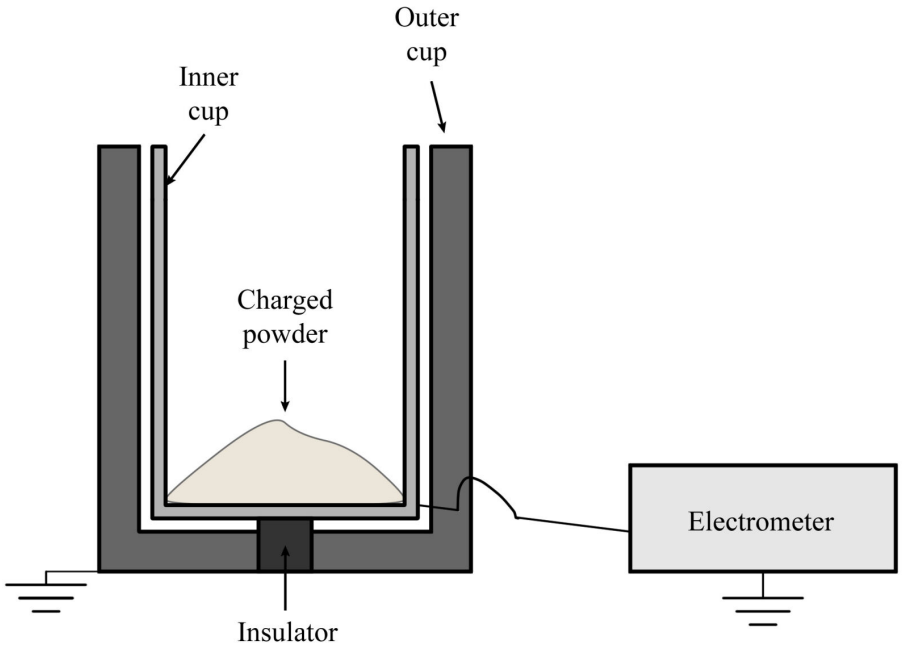

Figure 6: Labelled diagram of a Faraday cup

Food Particle Adhesion

Previous research has measured food particle adhesion following electrostatic charge generation. A study by Ricks et al. (2002) evaluated the impact of food powder characteristics

(size, charge, density, and flow index) on coating efficiency of corona charged particles. It was found that electrostatically charging particles improved coating efficiency by 68%. Similarly, Mayr et al., compared corona and triboelectric coating methods for seasonings on graham crackers (Mayr & Barringer, 2006). Adhesion was measured using the centrifuge technique. Their research concluded that electrostatics improved transfer efficiency by up to 40% and that increasing particle size could lead to better adhesion. In a later study, Huang & Barringer (2012), studied the impact of powder resistivity, coating voltage, and relative humidity on adhering salt, starch, and cocoa powders to food substrates. Charging of the powders was conducted using a corona charging powder spray gun and coating was done at up to 95 kV. Adhesion was measured using the centrifuge technique. It was found that starch adhesion increased with increasing coating voltage. Additionally, for electrostatically charged samples, the adhesion decreased when RH increased from 30 to 60%.

A study by Salazar et al. (2007), measured the adhesion of manioc starch on a steel surface using the centrifuge method. Practical results were also compared to the theoretical results. It was found that larger particles exhibited higher starch retention rates, and that the theoretical calculations predicted lower adhesion values than were measured experimentally. This was attributed to the small roughness, deformability, and organic composition of the particles.

A study by Peltonen et al. (2018), measured the electrostatic charge build-up of pharmaceutical powders, including starch, during their processing. The study simulated and measured tribo-charging by sliding powders down pipes of different materials and capturing them in a Faraday cup to measure both charge and mass. This process was repeated to chart the relationship between charge accumulation and mass. The study found that as particles became

adhered to the inner wall of the pipe, charge transfer to the powders decreased. Specifically, starch in contact with steel exhibited an average charge to mass ratio of -17.7 nC/g. This ratio diminished to -7.2 nC/g after the inner surface of the pipe was coated by the powder.

MATERIALS AND METHODS

To achieve the goal of this study, overall experimentation was structured into three key phases: (1) measuring the triboelectric charge build-up in flour samples under different relative humidity (RH) conditions, (2) quantifying the adhesion of flour particles on stainless steel coupons using abrupt deceleration forces, and (3) investigating the effect of vacuum treatment angle on cleanliness of flour-coated coupons. Specifically, the flour was milled from raw wheat kernels to maintain uniformity in particle size. For comparison between theoretical and measured adhesion forces, parameters such as electrostatic charge, deceleration rates, vacuum pressure, and air velocity were measured for their respective tests.

Flour Milling

Organic hard red winter wheat and soft white wheat berries/kernels were purchased from an online retailer (Palouse Farms, WA, USA). To replicate an all-purpose flour blend, an 80:20 ratio of hard red winter wheat and soft white wheat were used for milling (Bakerpedia, 2020). A KitchenAid mixer (Model K5-A, KitchenAid, Troy, OH, USA) with a grain milling attachment was used to grind the wheat berries into wheat meal. The milling attachment was set to the finest setting (notch 10) for all experimental runs and milled at mixing speed 4 (~125 rpm).

Figure 7: KitchenAid mixer with grain milling attachment

21 CFR requires that 98% of wheat meal particles must pass through a US Standard No. 70 mesh (>212 µm) to be classified as flour (Title 21, 1977). However, not all flour during processing may meet this final requirement. Thus, two particle size categories were selected to account for flour particles reasonably larger or smaller than the 21 CFR requirement, US Standard 60 – 80 mesh (diameter 250 – 177 µm), and US Standard 80 – 100 mesh (diameter 177 – 149 µm). To achieve this, the wheat meal was sieved through US Standard meshes No. 20, 60, 80, and 100 for 15 minutes to separate and refine the flour particles. A sieve shaker (Model H-4325, Humboldt, Elgin, IL, USA) was used to promote flour movement through the sieves. All particles that did not pass through the No. 20 mesh or passed through the 100 mesh were discarded. Flour particles that passed through meshes No. 60 or through No. 80 were kept

separated for further experimentation. Flour was stored within the humidity-controlled chambers at ambient humidity and temperature for up to a week before conditioning.

Figure 8: Sieves and mechanical sifter for flour particle size separation

Sample Conditioning

The prepared flour samples, 60 – 80 mesh and 80 – 100 mesh, were spread in a thin layer (< 2.5 cm) over separate quarter sheet pans (24 × 33 cm) to be equilibrated in a custom-built humidity control chamber (69 × 51 × 51 cm) for 24±2 hr before testing. The humidity control chambers were assembled to the specifications outlined by Smith et al. (2015).

Figure 9: Flour spread in quarter sheet pans for equilibration

Samples were equilibrated at 20, 40, and 60% RH. Successful equilibration of flour samples to the target relative humidity was verified with a water activity meter (Model 4TE, Decagon Devices, Pullman, WA, USA).

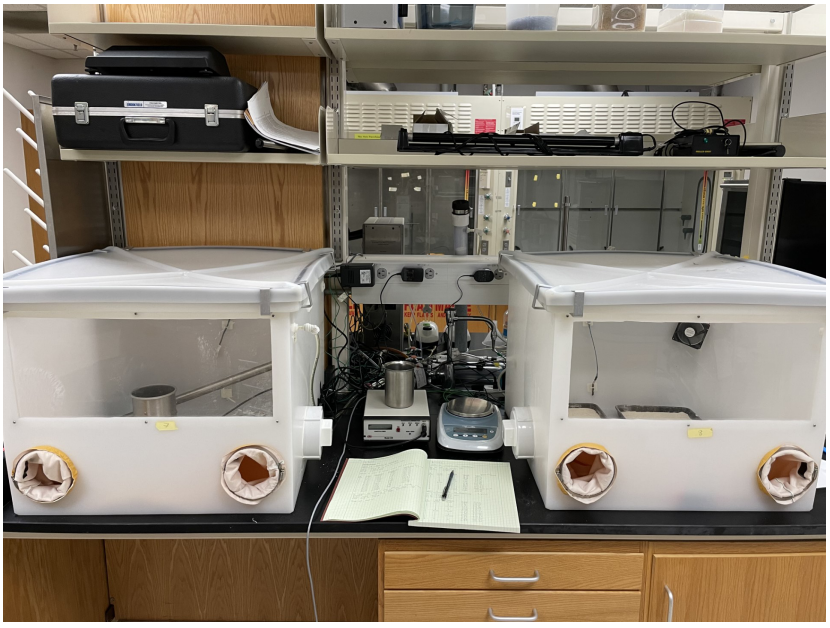

Figure 10: Custom humidity control chambers

Stainless Steel Coupons

To simulate low-moisture food contact surfaces, a series of electropolished grade 304 stainless steel coupons (8 × 8 × 0.2 cm) were fabricated, as described by Benoit et al., (Benoit, 2013). Before each use, coupons were cleaned to reduce presence of debris, residues, and bacteria using methodology modified from Suehr (2020). Coupons were submerged in an acetone bath for 15 minutes then left to air dry. They were then submerged in deionized water for 1 minute and dried within an oven (>100 °C) to evaporate any moisture on the surface and prevent rusting.

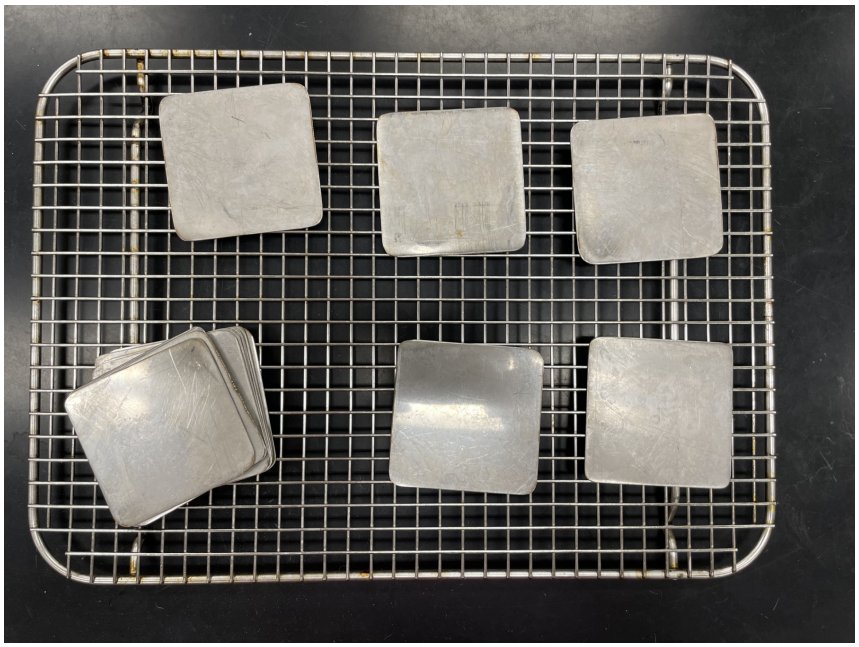

Figure 11: Custom electropolished grade 304 stainless steel coupons

Triboelectric Charge Generation

Preliminary experimentation used a rotating (0.8 rad/s) stainless steel drum (280 mm depth, 220 mm diameter) to charge silicon quartz powders triboelectrically. Thereafter, charge generation within the agitated powders was measured using a handheld digital electrostatic fieldmeter (FMX-003, Simco, Hatfield, PA, USA). However, due to the size limitations of the

humidity-controlled chambers, the rotating drum methodology was dismissed in favor of a more compact design that could agitate the powders at a faster rate. To achieve this a powder charging blender was constructed and tested.

The blender consisted of a quart paint can (946.35 ml, 10.16 cm diameter) housing an aluminum mixing blade (10.16 cm diameter) inside. An antistatic polyethylene shaft connected the mixing blade to the compact AC gear mount motor that facilitated rotation (up to 150 rpm). The shaft was made of nonconductive material to prevent charge dissipation from the can. The rotational speed was adjustable via a speed-controller connected to the power input of the motor. To charge the flour samples, flour was placed inside the can and the motor turned on to spin the mixing blade. During operation, as the flour collided with the mixing blade, walls of the can, and other flour particles, triboelectrification occurred, leading to charge build up within the sample. By manipulating the blender's rotational speed and duration, it was anticipated that varying levels of electrostatic charge could be imparted to the flour sample.

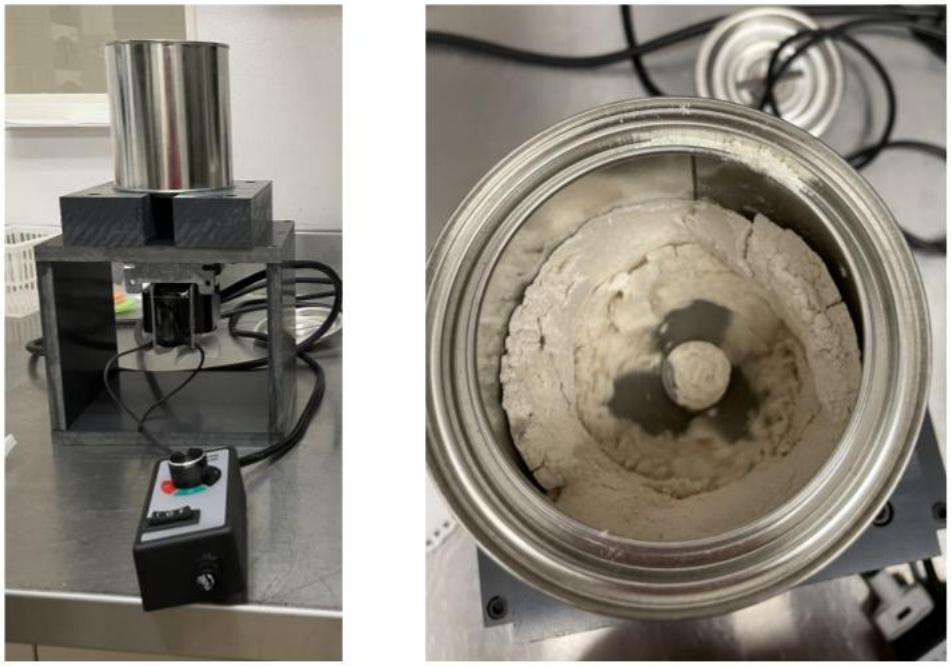

Figure 12: Custom built powder charging apparatus

However, the powder charging blender proved impractical and did not achieve the expected results. When in use, a portion of flour was often be pushed to the sides of the can and rest above the mixing blade, providing uneven charge. Nevertheless, charge generation within the can was confirmed using an electrostatic field meter. However, when charged flour was transferred via a plastic teaspoon to a Faraday cup for more precise charge measurements, there was no detectable difference in charge from a negative control sample. It was speculated that contact with the plastic spoon and time taken to transfer flour from the can to the Faraday cup caused most accumulated charge to dissipate before it could be measured. However, this trend continued even when charged flour was poured directly from the blender into the Faraday cup. Regardless, the powder charging blender proved ineffective, and a different approach was researched and developed.

Drawing on insights from a prior study (Peltonen et al., 2018), a simpler and more effective method for the tribocharging of powders has been identified using a charging pipe or tube. To replicate the process of triboelectrification that can occur when a powder flows through a pipe or any confined space, a stainless steel pipe (60 cm length, 3 cm interior diameter) was used. Flour was introduced to one end of the pipe using a quarter teaspoon (1.2 ml). Subsequent manual shaking of the pipe facilitated the movement of powder, inducing triboelectric charging as the powder slid and tumbled along the length of the pipe. The resulting electrostatically charged flour was then directly collected as it exited the opposite end of the pipe. To maintain consistency and remove flour build-up, the interior of the pipe was brushed with a pipe cleaner 10 times along its entire length between sample trials.

Figure 13: Stainless steel powder charging tube

Chargeability Tests

The chargeability tests were conducted inside the controlled humidity chambers to maintain a consistent relative humidity during the tribocharging process. Charge measurements were taken using a nanocoulombmeter (Model 230, Electro-Tech Systems, Perkasie, PA, USA) with a Faraday cup attachment (Model 231 Cup, Electro-Tech Systems, Perkasie, PA, USA). For charged samples, flour exiting the stainless steel charging tube was allowed to fall directly into the mouth of the inner Faraday cup. In contrast, uncharged flour samples at rest were transferred into the Faraday cup using a grounded stainless steel quarter teaspoon (1.2 ml).

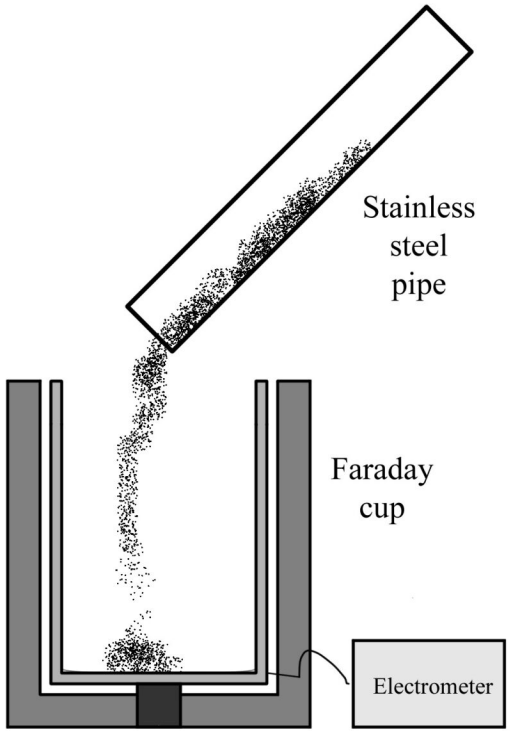

Figure 14: Powder charge measurement procedure using stainless steel tube

After recording of the charge values, the inner Faraday cup was removed from the equilibrium chamber, and the combined mass of the cup and flour sample was measured using a precision scale (Model S1002, Veritas, Santa Clara, CA, USA). The inner cup was then brushed until visually clean of flour particles before the next charge sample. The mass of the flour sample was determined by subtracting the known of the inner Faraday cup from the combined mass of the sample and inner cup, and this value was then used to calculate the charge-to-mass ratio (nC/g) for comparison with other samples. Chargeability tests were conducted in triplicate and utilized a full factorial design including factors relative humidity (20, 40, 60%), particle size (60 – 80, 80 – 100 mesh), and charge state (charged or uncharged).

Surface-Particle Adhesion

Before conducting adhesion or vacuum test, flour was applied to the stainless steel coupons. To facilitate this, each coupon was grounded using a grounding cable and placed on a custom wire easel which suspended the coupon above the surface of the humidity control chamber at a constant 60-degree angle. For charged flour samples, a quarter teaspoon (1.2 ml) of flour exiting the charging tube was allowed to freely flow from the top to bottom of the coupon, coating its surface with flour particles. For uncharged flour samples, a stainless steel quarter teaspoon was used to transfer flour at rest and directly disperse it over the coupons surface, freely flowing from the top to bottom of the coupon. After the coating process, the coupon was removed from the easel and grounding cable, then gently inverted to remove any loosely adhered particles.

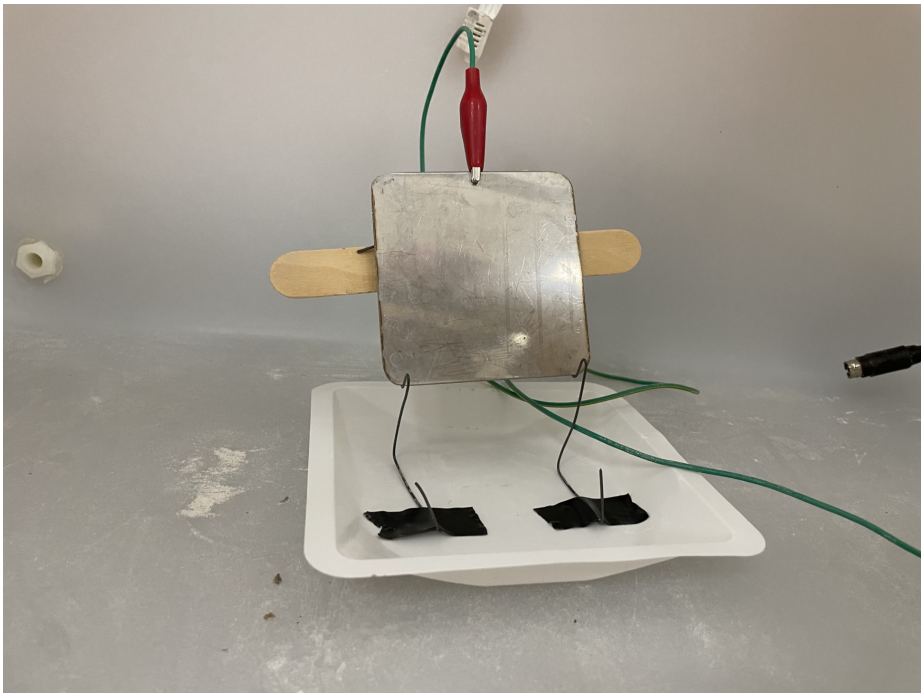

Figure 15: Custom wire easel with grounded stainless steel coupon before coating

Adhesion Tests

Several methods to quantify the adhesive force of flour particles on stainless steel surfaces were considered and tested before choosing the most practical option. Initially, the centrifuge technique was evaluated, with preliminary experiments conducted on silicon quartz particles of various sizes (100, 400, 1250, 3000, and 5000 mesh) (Klug et al., 2022). The initial charge of the powders at rest was measured using a handheld digital electrostatic field meter. To enhance their static charge, a rotating stainless steel drum was used to agitate the powders for 10 minutes. Then, 3 g of each powder was evenly distributed over 304, mirror finish stainless steel coupons (10 mm x 10 mm) and subsequently centrifuged at 119.5 × g for 1 min in the centrifuge sample holder. A custom sample vial was designed to hold the coupons 10 mm from the bottom of the centrifuge vial and perpendicular to centrifugal force, following the method described by Suehr (2020). After the centrifuge test, the mass of powder that had been dislodged from the coupon surface was weighed, three trials conducted for each combination of mesh size and charge.

While the centrifuge tests showed promising results, they also highlighted several limitations. Firstly, relative humidity, a critical factor in electrostatic charge generation and retention, could not be controlled for the tests. Furthermore, the interval between charging the silicon powder, coating the coupons, and conducting the centrifuge test was often protracted, increasing likelihood of charge dissipation before adhesion tests could start. Additionally, the small surface area of the stainless steel coupons used in the centrifuge vials restricted the amounts of powder that could be adhered, making it difficult to detect the minute differences in mass. Collectively, these challenges rendered the centrifuge method unsuitable for the intended experiment.

The possibility of measuring bulk flour adhesion and cohesion was also explored. To achieve this, a methodology was adapted and modified from Chen et al., 2022, to measure the shear force required to pull a ring filled with flour across a stainless steel surface. To measure and record the shear force curves, a texture analyzer (TA.HD.Plus, Stable Micro Systems, Godalming, Surrey, UK) was utilized to apply consistent speed and movements. The texture analyzer consists of a 5 kg load cell attached to a programmable arm that can raise and lower the load cell for set distances and speeds. A custom-design pulley system was mounted below the load cell, where a string was fed through the pulley with one end attached to the load cell and the other to the stainless steel ring (0.5 in height, 1 in diameter). As the arm rises, the powder filled ring would be pulled across the coupon surface and the texture analyzer would record the shear force required to do so. To control for relative humidity, the string attached to the ring could be run through a small hold in the humidity-controlled chambers for experimentation within the chambers. After testing the methodology, it quickly became apparent that the load cell for the texture analyzer was not sensitive enough to detect the minute differences in adhesion caused by electrostatic forces. Additionally, applicability of bulk flour adhesion measurements to real-life scenarios, where powders are more dispersed over a surface, was also called into question. Consequently, it was decided to move forward with an alternative adhesion measurement methodology.

The final adhesion measurement methodology tested to quantify the adhesion force of the flour particles on the stainless steel coupons involved an impact adhesion tester (IAT) (Ermis et al., 2011). The IAT offered advantages over other adhesion quantification methods, such as centrifugation, including its compact size, which allows for placement inside controlled humidity chambers, and its capacity to perform swift, consecutive tests.

The IAT works by using removal forces to detach particles from a coupon surface through its rapid deceleration. This deceleration occurs when the coupon is dropped from a height and hits the ground. The impact halts the coupon, but the particles, due to inertia, keep moving unless held by adhesion forces. The removal force on each particle depends on its mass and acceleration, with the particle's acceleration being equal to the coupon's deceleration at impact. If the removal force exceeds the adhesion forces, the particles will be dislodged from the coupon.

The IAT was constructed by the Department of Biosystems and Agricultural Engineering Fabrication Shop (Michigan State University, East Lansing, MI). It features a smooth stainless steel rod (43 cm length, 2.5 cm diameter) positioned at a 90-degree angle on an aluminum base (30 × 15 × 4.5 cm). A flat-faced linear ball-bearing carriage (TWA16WUU, Nippon Bearing, Hanover Park, IL, USA) is designed to slide up and down the rod. A square steel frame (Outer dimensions: 10 × 10 cm, inner dimensions: 7.5 × 7.5 cm) was fabricated to hold the coated coupon samples and attached perpendicularly to the face of the ball-bearing carriage. Two rubber stoppers were drilled into the bottom of the frame to cushion the descending carriage. An adjustable ring was added above the carriage to regulate drop heights.

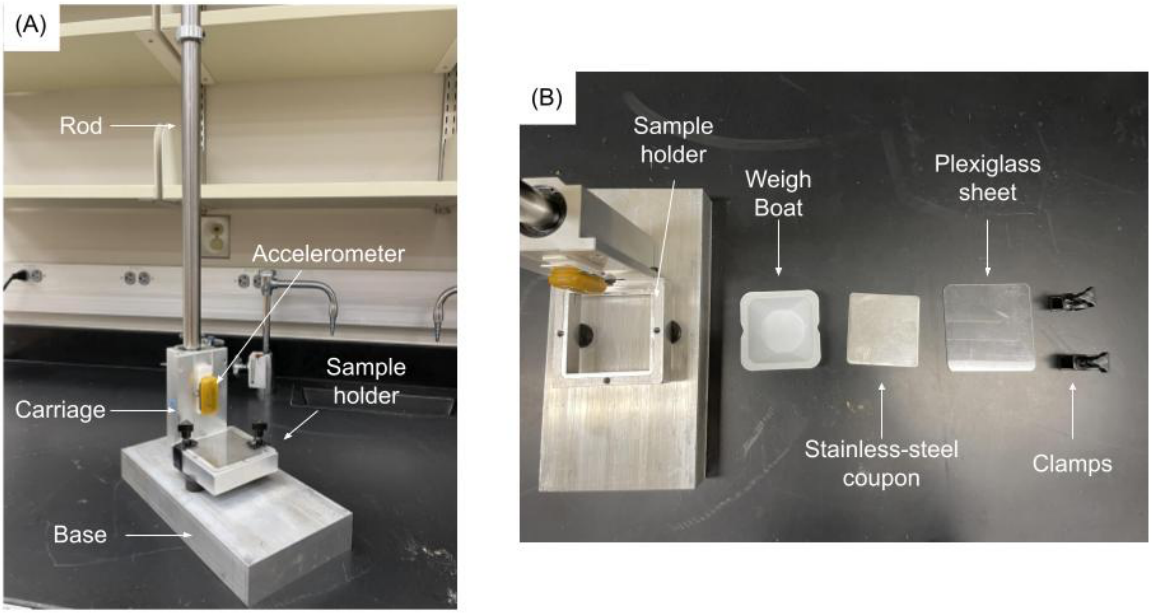

Figure 16: (A) Labelled diagram of IAT, and (B) Labelled diagram of sample holder components

To load the IAT, the flour coated coupons (coated using charging tube or grounded quarter teaspoon) were positioned face down over a small plastic weigh boat. Subsequently, both coupon and weigh boat were transferred to the steel frame of the IAT. A plexiglass covering was placed on top of the coupon, and clamps were applied to either end of the frame to hold everything in place.

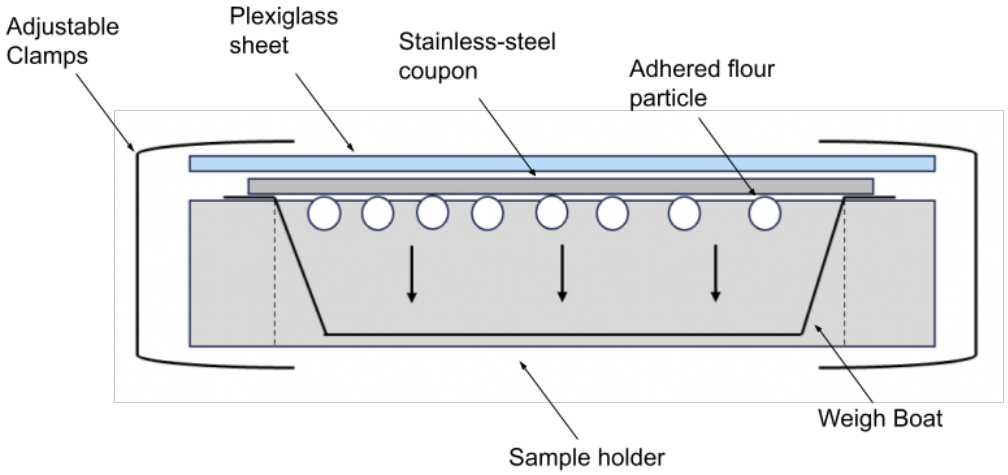

Figure 17: Labelled diagram of an assembled sample holder

A compact accelerometer (MSR175, MicroDAQ, Concord, NH, USA) was affixed with epoxy to the face of the carriage above the sample holder frame. The accelerometer was programmed to measure shock events greater than 1 g. The shock/impact data were processed using analysis software package MSR ShockViewer, then exported to Excel spreadsheet format. To assess the replicability and relationship between drop height and deceleration, the carriage was dropped from heights ranging from 2.5 – 25 cm in triplicate. Based on the calibration data, drop heights of 2.54, 12.70, and 22.86 cm were selected for use in the adhesion tests. These three drop heights were chosen to represent the range of deceleration forces able to be applied by the IAT, and because each height provided a distinct deceleration value with no overlap with the other two heights. For each trial, deceleration values were recorded to ensure alignment with the calibration curve.

All impact adhesion tests took place inside the controlled humidity chamber. For each flour-coated coupon, once positioned facedown in the IAT sample holder, the carriage was elevated to its specified height (2.54, 12.70, or 22.86 cm) before being released. As the carriage falls and impacts the base, the force of the impact acts normally against the force of adhesion and dislodges particles from the surface. The flour particles dislodged from the impact fall into the weigh boat below. Following the impact test, the coupon and weigh boat are carefully removed from the sample holder and equilibrium chamber for weighing.

Mass measurements were conducted using an analytical balance (Model E12140, Explorer, Ohaus, Parsippany, NJ, USA). The mass of the adhered flour and coupon were measured, and then the mass of the weigh boat and dislodged flour. By subtracting the known mass of the individual coupon and weigh boat, the percentage of flour remaining adhered can be calculated for comparison between samples. Impact adhesion tests were conducted in triplicate

and with a full factorial design including factors, like relative humidity (20, 40, 60%), particle size (60 – 80, 80 – 100 mesh), charge state (charged or uncharged) and drop height (2.54, 12.70, or 22.86 cm).

Vacuum-Cleaning Tests

Vacuum-cleaning treatments were applied using a compact handheld vacuum device (Model 47R5-1, Bissell, Walker, MI, USA). This handheld unit was preferred over a larger shop-vac to ensure it could fit entirely inside the humidity-controlled chambers, maintaining the relative humidity level undisturbed during operation. Using a clamp and a ring stand, a round vacuum nozzle (3.81 cm diameter) with no attachments was positioned above the horizontally placed, face-up coated coupons. The nozzle's base was set 1.3 cm above the surface of the coupon and its angle was adjusted with a protractor to 0, 45, and 90 degrees relative to the coupon surface.

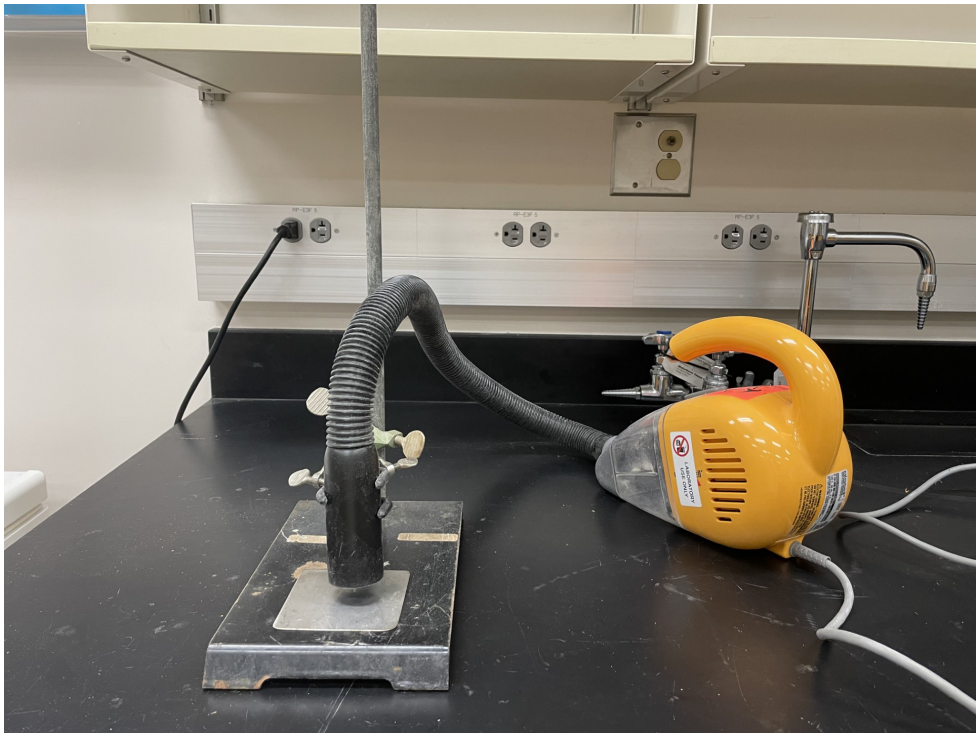

Figure 18: Handheld vacuum unit with ring stand

To quantify the removal force exerted by the vacuum treatment at various angles, a digital hand-held manometer (Series 477AV, Dwyer, Michigan City, IN, USA) was utilized. A digital manometer has two ports leading to pressure transducers. An elastic portion of the transducer is capable of measuring and converting pressure levels into electronic signals. One manometer port was open directly to the atmosphere while the other port was attached to a rubber elastic tube (3.18 mm interior diameter). The other end of the tube was positioned directly at the surface of the stainless steel coupon, below the vacuum nozzle. By measuring the pressure at each of the ports, the digital manometer could calculate the pressure differential at the coupon surface caused by the vacuum treatment. Additionally, the digital manometer is capable of automatically calculating the air velocity of the vacuum treatment based on the measured pressure differential. To accurately portray the entire range of pressure or air velocity acting on a particle at the coupon surface, the rubber tube of the manometer was adjusted and repositioned to different points along the coupons surface: center, edges, and directly below vacuum nozzle. The manometer was programmed to record the minimum and maximum pressure and air velocity values induced by each nozzle angle treatment.

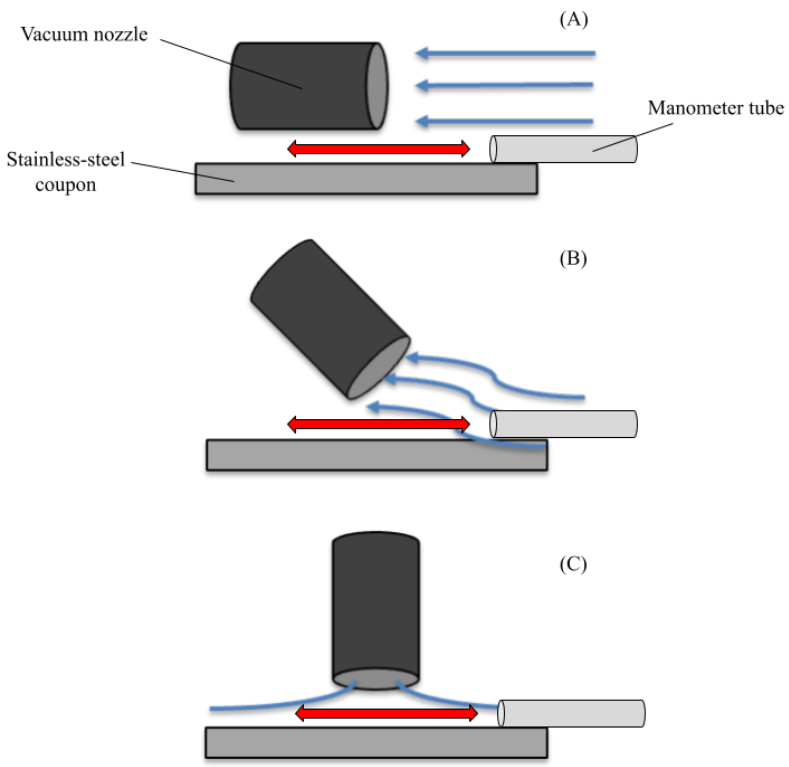

Figure 19: Vacuum nozzle and manometer tube placement for (A) 0 degrees, (B) 45 degrees, and (C) 90 degrees

The small handheld vacuum unit used for experimentation is expected to apply lower pressure and air velocity to surfaces being cleaned when compared to commercial units used for industrial cleaning. To characterize this difference, the digital manometer was used to measure the pressure differential and air velocity supplied at coupon surfaces by a 4 horsepower, mobile, 8 gallon wet/dry vacuum cleaner (Model 125.17608, Craftsman, Hoffman Estates, IL, USA). Measurements were taken using the same procedures described for the handheld unit, and the nozzle angle was kept at 90 degrees relative to the coupon surface.

All vacuum-cleaning tests occurred within the humidity-controlled chamber. When positioned correctly, the vacuum was turned on, and the coated coupon was manually moved below the nozzle to ensure maximum removal forces were applied to all areas of the coupon surface. Once surface appeared visually clean of residue, the vacuum was turned off and the

stainless steel coupon was removed from the humidity-controlled chamber for ATP assay. Typical vacuum cleaning treatments lasted approximately 10 seconds before the surface appeared visibly clean.

Cleanliness of the coupon surfaces following the vacuum treatments were conducted using ATP swabs (Ultrasnap, Hygiena, Camarillo, CA, USA) and a luminometer (SystemSURE plus, Hygiena, Camarillo, CA, USA). Although ATP is an organic compound found in all living things, such as bacteria, plant cells, and animal cells, ATP assay cannot differentiate between sources. However, due to the acetone and deionized water rinsing of the coupons before coating, it can be reasonably assumed that the majority of ATP recovered from coupon surfaces resulted from flour. Coupon surfaces were swabbed in accordance with the manual provided by the manufacture (Hygiena SystemSURE plus). Surfaces were swabbed horizontally, then vertically while rotating and pressing with the surface swabs to cover the entire area of the coupon. ATP collected on the swabs react with an enzyme within the swab holder, generating light, which the luminometer quantifies in Relative Light Units (RLU) for comparison between vacuum-cleaning treatments. Vacuum-cleaning tests were conducted in triplicate and with a full factorial design of factors, relative humidity (20, 40, 60%), particle size (60 – 80, 80 – 100 mesh), charge state (charged or uncharged) and nozzle angle (0, 45, 90 degrees). For reference, RLU values were also recorded for “clean” coupons (i.e., negative control) and unvacuumed coated coupons (i.e., positive control) in triplicate for comparison.

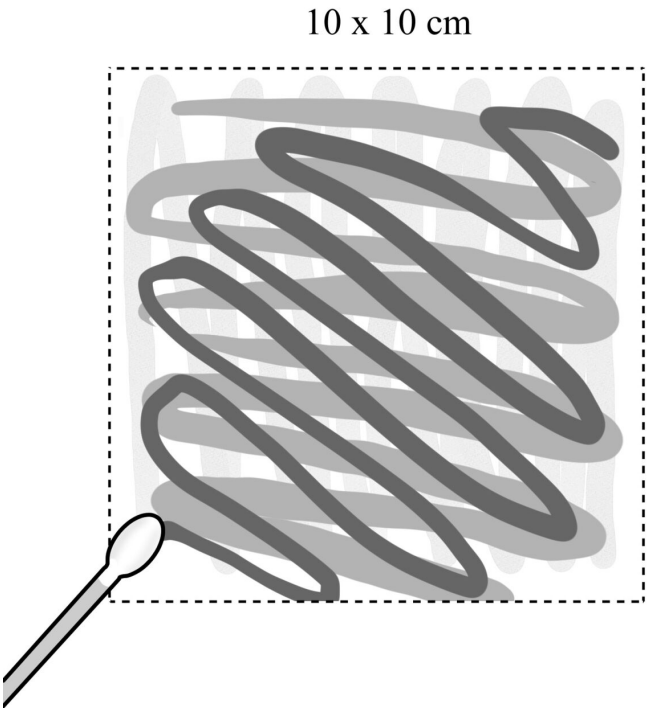

Figure 20: Recommended swabbing technique

Statistical Analysis

Data analysis was conducted using statistical analysis software Minitab (Minitab 21, State College, PA, USA). The data normality and variance for each experimental segment (chargeability, impact adhesion, and vacuum) was analyzed to ensure analysis of variance (ANOVA) could be conducted. The normality assumption was checked through examining a histogram, q-q plot and residual vs. predicted plots. As no variances from normality were found, there was no need to transform the data. The unequal variance assumption was checked by visual inspection of side-by-side box plots of each fixed factor and their interactions, followed by Levene's test for unequal variance.

After ensuring that the data were distributed normally and variances were equal, data were analyzed for each experimental segment using the general linear model (GLM) procedure for ANOVA. GLM is used to determine whether the means of two groups are significantly

different (α=0.05). A least squares regression calculation is used to predict the statistical relationship between multiple predictor factors and the continuous measured response value. The factors of relative humidity, charge, size, drop height and vacuum angle were analyzed as categorical values rather than numeric. Through the ANOVA calculation, the statistical significance of individual factors and their interactions with other factors could be determined.

Following the ANOVA, all pairwise comparisons using Tukey's test for means were conducted (α=0.05). Tukey's test was used rather than a traditional t-test to control for the increased chance of type 1 error caused by multivariate comparisons. To better discern trends influenced by numerous factors (relative humidity, particle size, charge state, drop height, nozzle angle), data slicing was employed for both the adhesion and vacuum-cleaning tests. Slicing divides the dataset along factor lines so that data can be analyzed separately within different categories. Data for adhesion tests was sliced by factors mesh size and force of removal, while data for vacuum tests was sliced by factors mesh size and relative humidity. After slicing, once again pairwise comparisons of means were conducted using Tukey's test (α=0.05).

CALCULATIONS

Practical results for adhesion and cleanability of flour from surfaces can be better understood through comparison with theoretical models. Furthermore, the applicability of theoretical equations to real-life situations can be evaluated through such a comparison. Several more nuanced and complex models for predicting particle adhesion on a surface have been proposed (Butt, 2008; Cheng et al., 2002; Rabinovich et al., 2002; You & Wan, 2013, 2014). However, to match the scope of the experiment, only the following fundamental equations were used.

Adhesion Force Equations

The total adhesion force causing a particle to stick to a surface is the cumulative effect of Van der Waals, electrostatic, and capillary forces on the particle. Depending on the properties of the particle, substrate, and environment, one or more of these forces may be dominant over the others. Total adhesion force is expressed in Eq (1):

$$F_{ad} = F_{vd} + F_{es} + F_c \tag{1}$$

where F_{ad} is the total force of adhesion, F_{vd} is the Van der Waals force, F_{es} is the electrostatic force, and F_c is the capillary force. In low-moisture environments, the amount of adhesion provided by capillary forces can be assumed to be negligible due to the lack of moisture in the environment.

Van der Waals forces are weak intermolecular forces of attraction or repulsion between atoms or molecules. Assuming a spherical particle, the Van der Waals force between a flour particle and a plate is given by Eq (2):

$$F_{vd} = \frac{Ar}{6h^2} \tag{2}$$

where A is the Hamaker constant, r is the radius of the particle, and h is distance between the particle and the target. As values for the Hamaker constant and distance between particle and surface cannot be measured, critical assumptions must be made. Thus, the Hamaker value for starch molecules, 5.2×10^{-20} J (Salazar-Banda et al., 2007) and the distance, h, ranging from 5×10^{-8} m (Ermis et al., 2011; Huang & Barringer, 2012) to 5×10^{-10} m (Salazar-Banda et al., 2007) can be used for the calculation.

Electrostatic forces within the food particles induce an equal and opposite charge on the grounded coupon surfaces. Coulombic law for a single spherical particle is given by Eq (3):

$$F_{es} = \frac{Q^2}{4\pi\varepsilon_0(r+h)^2} \tag{3}$$

where Q is the charge on a single particle, and ε_0 is the vacuum permittivity constant, 8.85×10^{-12} $C^2\ J^{-1}\ m^{-1}$. The charge, Q, can be calculated through the measured charge to mass ratio values from the chargeability tests and the estimated mass of a single particle, as described in Eq (4):

$$Q = qm_p \tag{4}$$

where q is the measured charge to mass ratio (nC/g) and m_p is the calculated mass of a single spherical particle, inferred from known range of mesh size diameters and the estimated density of an individual particle, assumed to be similar to the true density of wheat grain: 1395 kg/m^3 (Aremu et al., 2014).

Force Equations for IAT

The total force of removal acting on the adhered particles during the IAT tests is given by Eq (5):

$$F_{rem} = F_i + F_g \tag{5}$$

where F_{rem} is the total force of removal, F_i is the force of the impact, and F_g is the force of gravity. The force of gravity can be calculated given Eq (6):

$$F_g = m_p \alpha \quad (6)$$

where α is the gravitational acceleration, 9.8 m/s^2.

The force of impact provided by the IAT can be calculated using Eq (7):

$$F_i = m_p \alpha_i \quad (7)$$

where α_i is the average deceleration value measured by the accelerometer during testing.

RESULTS

Preliminary Tests

Preliminary experiments utilized silicon quartz powders to evaluate a rotating drum tumbler for charging and the centrifuge method for measuring adhesion. The average percentage loss difference between each mesh size for control and charged groups was calculated. To compare the electrostatic charge before and after tumbling, a 95% confidence paired t-test was applied. On average, "the powders of mesh sizes 400, 1250, 3000, and 5000 retained 2.21, 5.38, 23.81, and 5.62% more respectively after being tumbled and electrostatic charges (0.07, 0.60, 0.50, and 0.83 kV) were increased. However, the largest mesh size (100) powder was retained 18.53% less after being tumbled (0.81 kV)" (Klug et al., 2022). For all powders, electrostatic charge was significantly greater following the tumbling treatment ($P < 0.01$).

Water Activity Measurements

Water activity of the flour samples after 24±2 h within the humidity-controlled chambers was measured to ensure samples were reaching the target moisture level. Average water activity of the flour samples successfully reached within ±3% environments target relative humidity (Table 1).

Table 1: Water activity of flour samples after equilibration

Target relative humidity (%)	Water Activity (%)	
	Mesh size	Mean ± SD
20	60 – 80	21.32 ± 2.84
	80 – 100	18.56 ± 3.03
40	60 – 80	40.06 ± 1.87
	80 – 100	40.48 ± 2.09
60	60 – 80	58.69 ± 0.32
	80 – 100	60.63 ± 2.14

Chargeability Factors Analysis

Analysis of variance using the general linear model was conducted through Minitab statistical software. The impact of relative humidity, mesh size, treatment, and all possible combinations of interactions were tested for significant impact on the resulting electrostatic charge (α=0.05). The factors of relative humidity and treatment (charged or uncharged) were significant, whereas mesh size and all its interactions were found to have a negligible impact on the measured charge-to-mass ratio (Table 2).

Table 2: ANOVA for chargeability factors and their interactions

Source	Degrees of Freedom	Adjusted Sum of Squares	Adjusted Mean Squares	F-Value	P-Value
Relative Humidity	2	23.870	11.935	39.74	0.000
Mesh Size	1	0.009	0.009	0.03	0.863
Treatment	1	113.514	113.514	377.95	0.000
Relative Humidity*Mesh Size	2	0.266	0.133	0.44	0.647
Relative Humidity*Treatment	2	20.441	10.221	34.03	0.000
Mesh Size*Treatment	1	0.126	0.126	0.42	0.524
Relative Humidity*Mesh Size*Treatment	2	0.070	0.035	0.12	0.891
Error	24	7.208	0.300		
Total	35	165.504			

Following the ANOVA, all pairwise comparisons were conducted using Minitab statistical software. Grouping was conducted using the Tukey method with 95% confidence

intervals. For the uncharged flour sample controls, no significant difference in charge was observed between different relative humidity values and particle size distributions (Figure 21). Triboelectrically charged flour samples were significantly higher than control samples for each relative humidity and particle size (p values<0.001). There was no significant difference in charge generation between 60 – 80 mesh and 80 – 100 mesh particle distributions (p value=0.863). The charge to mass ratio for the charged flour samples at 20% relative humidity were significantly greater than both 40% and 60% charged values (p values<0.001).

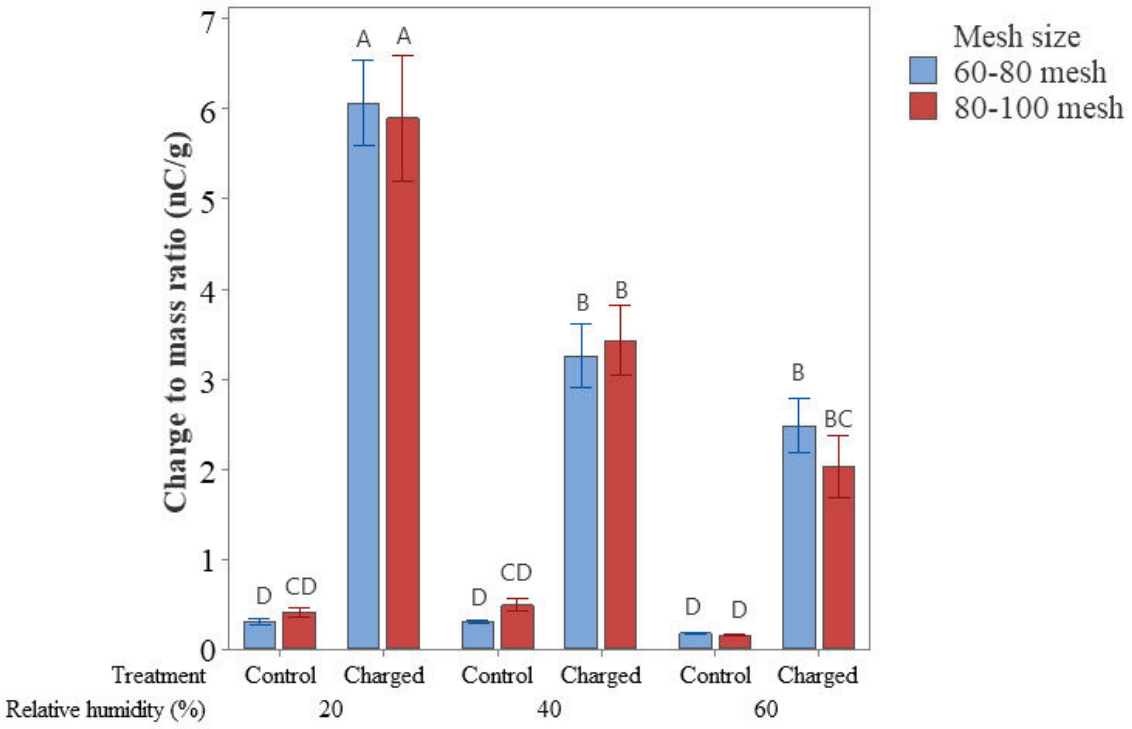

Figure 21: Mean charge-to-mass ratio values for charged and uncharged flour particles at different relative humidity values. Error bars are one standard error from the mean. Means sharing a common letter are not significantly different

Charge-to-mass ratio was not significantly influenced by particle size; therefore, mean values and standard deviations were calculated for charged particles based upon relative humidity. None of the control samples were significantly different from one another, so statistics were calculated for uncharged flour as a group (Table 3).

Table 3: Combined mean charge values for charged and uncharged flour samples at different relative humidity.

	Charge to mass ratio (nC/g)
Treatment	Mean ± SD
20% RH, charged	5.98 ± 0.93
40% RH, charged	3.34 ± 0.58
60% RH, charged	2.25 ± 0.56
Control	0.3 ± 0.13

Impact Adhesion Tester (IAT)

The force of removal acting on a particle is a product of the particle's mass and acceleration. The acceleration of the particle moving away from the coupons surface is equal in magnitude to the deceleration of the coupon during the impact. To ensure that the acceleration acting on the particles was consistent, a compact accelerometer was used to measure and characterize the deceleration of the IAT and coupon system.

To calibrate the IAT, a curve correlating drop height with peak deceleration values was established (Figure 22). The diminishing differences in deceleration values with increasing drop heights can likely be ascribed to the rail system nearing terminal velocity. Nonetheless, deceleration forces ranged from ~50 to ~170 g, and the confidence intervals of lower drop heights had little overlap. Therefore, unique deceleration forces could be applied consistently using the IAT.

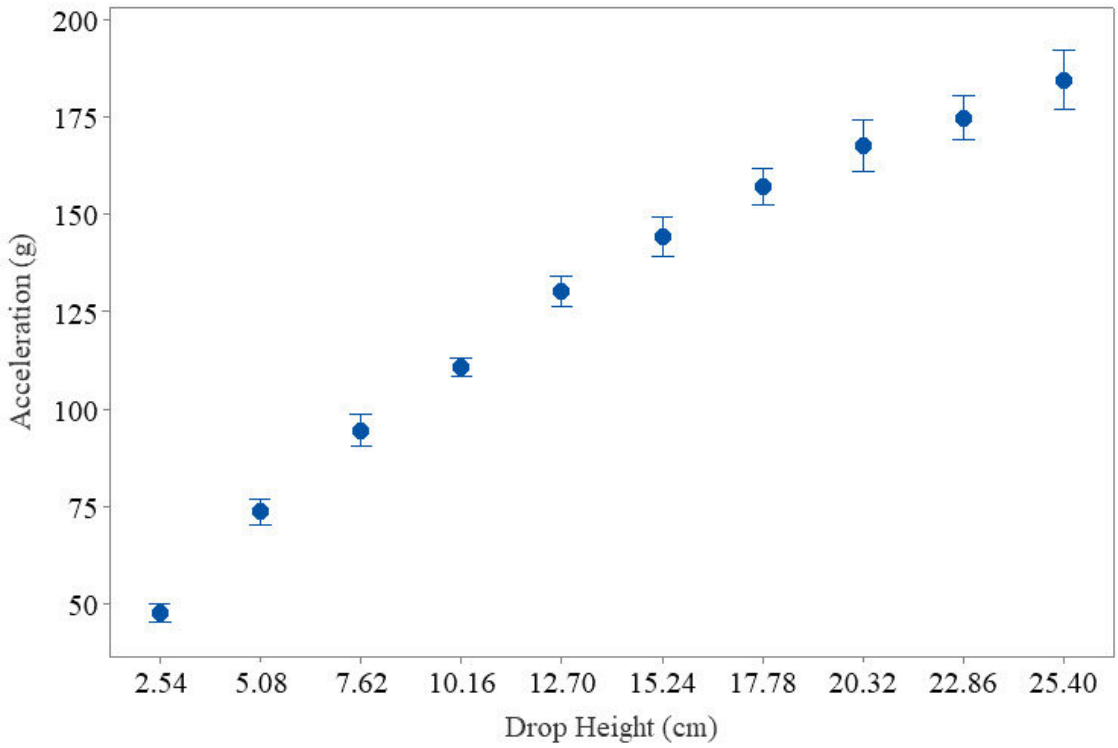

Figure 22: Drop height vs. deceleration. Error bars represent 95% confidence interval

The accelerometer was capable of recording not just the peak deceleration but also the deceleration history throughout the entire impact event. Figure 23 displays example shock event graphs recorded for each of the chosen heights for testing (2.54, 12.70, and 22.86 cm). For each drop height, it can be observed that a secondary, lesser deceleration peak follows the initial impact, resulting from the IAT carriage experiencing a slight bounce after the initial impact before coming to a complete stop. When calculating detachment forces, only the first peak was taken considered, with subsequent shocks deemed negligible (Ermis, 2011).

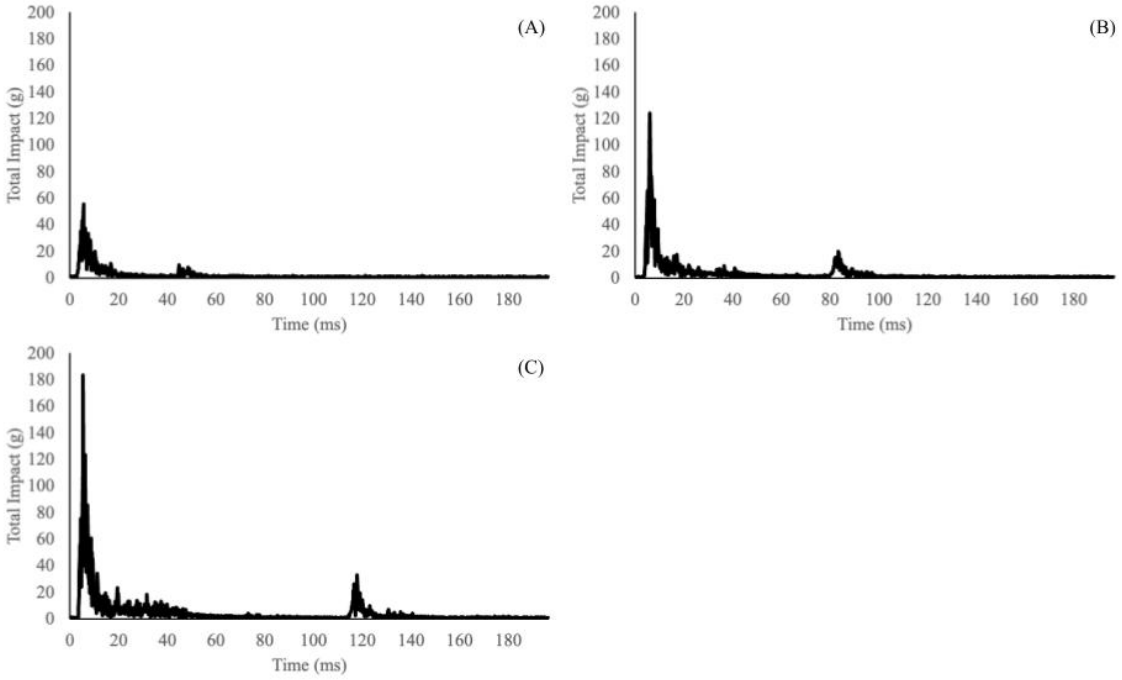

Figure 23: Example shock acceleration graphs for (A) 2.54 cm drop, (B) 12.70 cm drop, and (C) 22.86 cm drop

Adhesion Force Analysis

Analysis of variance using the general linear model was conducted through Minitab statistical software. The impact of relative humidity, mesh size, treatment, drop height and all possible combinations of interactions were tested for significant impact on the resulting flour retention rate (α=0.05). Relative humidity, treatment (charged or uncharged), and drop height (deceleration value) all had a statistically significant impact on their own, and mesh size was shown to be significant through its interactions (Table 4).

Table 4: ANOVA for adhesion factors and their interactions

Source	Degrees of Freedom	Adjusted Sum of Squares	Adjusted Mean Squares	F-Value	P-Value
Relative Humidity	2	2422.8	1211.39	37.97	0.000
Mesh Size	1	58.4	58.42	1.83	0.180
Treatment	1	3113.0	3112.99	97.57	0.000
Drop height	2	7776.0	3888.02	121.86	0.000
Relative Humidity*Mesh Size	2	224.8	112.40	3.52	0.035
Relative Humidity*Treatment	2	827.7	413.83	12.97	0.000
Relative Humidity*Drop height	4	209.1	52.27	1.64	0.174
Mesh Size*Treatment	1	672.6	672.57	21.08	0.000
Mesh Size*Drop height	2	274.4	137.20	4.30	0.017
Treatment*Drop height	2	134.3	67.14	2.10	0.129
Relative Humidity*Mesh Size*Treatment	2	166.7	83.35	2.61	0.080
Relative Humidity*Mesh Size*Drop height	4	329.9	82.47	2.58	0.044
Relative Humidity*Treatment*Drop height	4	174.1	43.51	1.36	0.255
Mesh Size*Treatment*Drop height	2	131.4	65.69	2.06	0.135
Relative Humidity*Mesh Size*Treatment*Drop height	4	62.5	15.61	0.49	0.743
Error	72	2297.1	31.90		
Total	107	18874.6			

Deceleration values, or shock values, were logged for each IAT sample by the accelerometer (Table 5). Despite being subjected to the same deceleration values, the force of

removal is dependent on particle mass. For each mesh size categories, average force values were calculated, assuming a normal distribution of particle sizes within the categories.

Table 5: Mean shock values from impact adhesion tester

Drop height (cm)	Shock (*g*) Mean ± SD
2.54	50.51 ± 3.94
12.70	117.96 ± 8.23
22.86	164.22 ±10.52

For coupons subjected to the IAT, data were sliced along particle size distributions to calculate and analyze the average applied removal force. For flour within the 60 – 80 mesh particle distribution, average applied removal forces were 3.90, 9.01, and 12.51 μN for 2.54, 12.70, and 22.86 drop height, respectively. Within each force category, percentage of flour retained was significantly higher for charged flour samples at 20% RH when compared to charged samples at 60% RH (p values < 0.001) (Figure 24). Additionally, within each force category, only two of the uncharged flour control samples differed in percentage from each other. There was no significant difference in adhesion results between charged and control flour samples at 60% RH (p value=0.493). Conversely, there was a significant difference between charged and control samples at 20% RH (p value < 0.001).

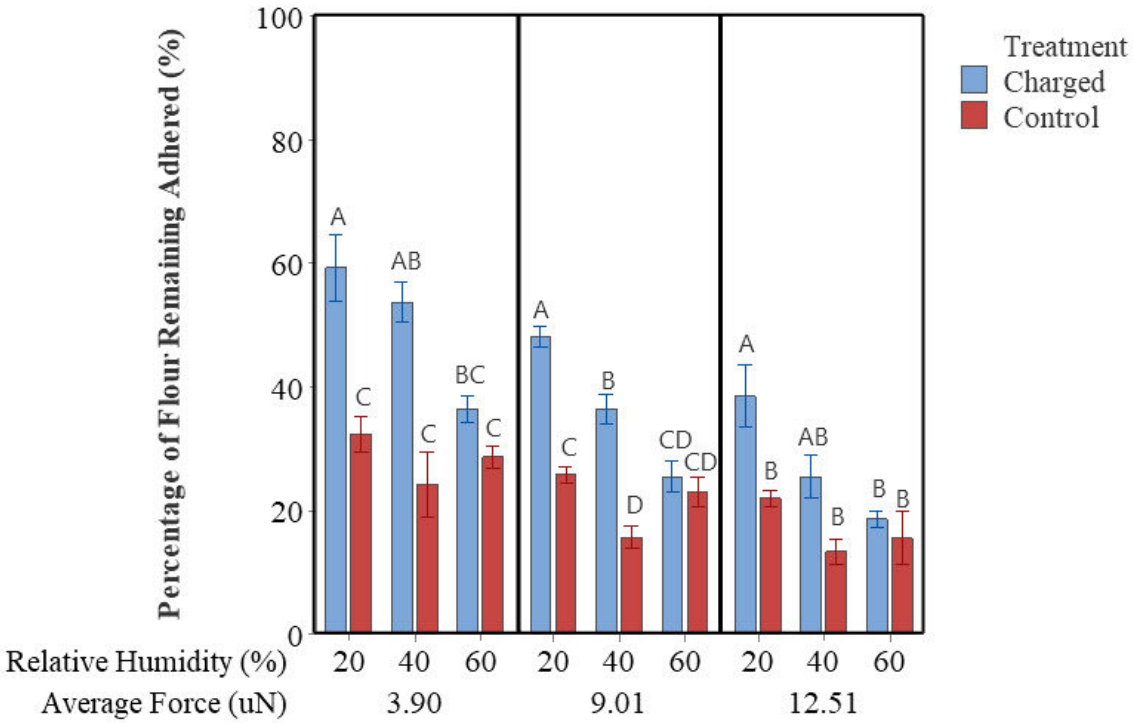

Figure 24: Comparison of powder retention rate by relative humidity and average force applied using an impact adhesion tests for 60 – 80 mesh wheat flour. Error bars are one standard error from the mean. Within a panel, means sharing a common letter are not significantly different

For flour within the 80 – 100 mesh particle distribution, average applied removal forces were 1.63, 3.77, and 5.23 µN for 3, 13, and 23 drop height, respectively. Within each force category, only 3.77 µN showed a significant difference between particle retention percentages for charged particles at 20% RH (Figure 25). All other retention percentages within a force category were not significantly different.

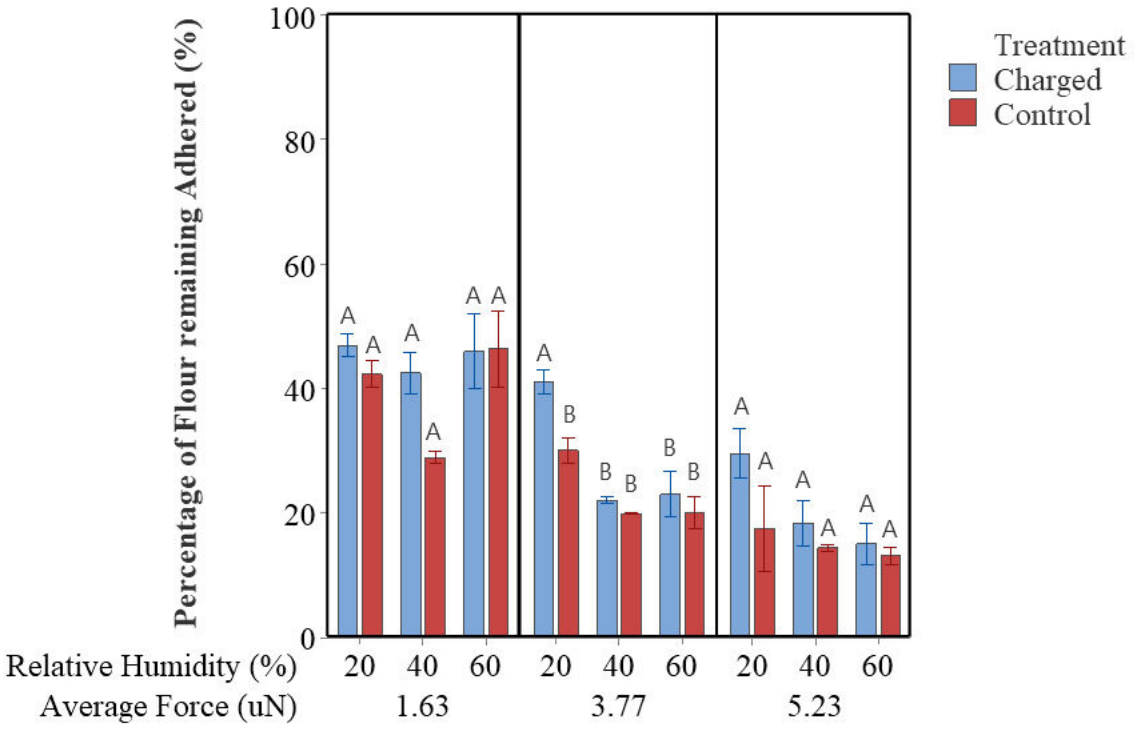

Figure 25: Comparison of powder retention rate by relative humidity and average force applied using an impact adhesion tests for 80 – 100 mesh wheat flour. Error bars are one standard error from the mean. Within a panel, means sharing a common letter are not significantly different

When analyzed without slicing of the data, the factor of deceleration (p value<0.001) and the interaction between particle size and deceleration (p value=0.017) were found to have a statistically significant impact on measured particle retention values (Table 4). The average percentage of flour that remained adhered was higher for larger particle sizes and decreased with lower deceleration values.

Vacuum-Cleaning

Analysis of variance using the general linear model was conducted through Minitab statistical software. The impact of relative humidity, mesh size, treatment, nozzle angle, and all possible combinations of interactions were evaluated for their significance on the cleanliness of the stainless steel coupon treated with vacuum cleaning (α=0.05). Relative humidity, treatment

(charged or uncharged), and angle of vacuum application all had a significant impact on ATP residues, whereas mesh size and all its interactions were found to be negligible (Table 6).

Table 6: ANOVA for vacuum cleanability factors and their interactions

Source	Degrees of Freedom	Adjusted Sum of Squares	Adjusted Mean Squares	F-Value	P-Value
Relative Humidity	2	4322.4	2161.19	18.94	0.000
Mesh Size	1	327.3	327.26	2.87	0.095
Treatment	1	3029.5	3029.48	26.55	0.000
Angle	2	6586.2	3293.08	28.86	0.000
Relative Humidity*Mesh Size	2	564.2	282.12	2.47	0.091
Relative Humidity*Treatment	2	244.7	122.34	1.07	0.348
Relative Humidity*Angle	4	761.1	190.28	1.67	0.167
Mesh Size*Treatment	1	62.3	62.26	0.55	0.462
Mesh Size*Angle	2	418.1	209.06	1.83	0.167
Treatment*Angle	2	60.8	30.40	0.27	0.767
Relative Humidity*Mesh Size*Treatment	2	11.8	5.90	0.05	0.950
Relative Humidity*Mesh Size*Angle	4	888.0	222.01	1.95	0.112
Relative Humidity*Treatment*Angle	4	203.0	50.76	0.44	0.776
Mesh Size*Treatment*Angle	2	133.4	66.68	0.58	0.560
Relative Humidity*Mesh Size*Treatment*Angle	4	242.3	60.56	0.53	0.713
Error	72	8214.7	114.09		
Total	107	26069.7			

ATP residues on the stainless steel surface were measured after vacuum cleaning until "visually clean" of flour particles. Cleaning treatments were applied at a standard height (1.3 cm)

above the surface with varied angles (0, 45, 90 degrees). The vacuum force at the surface of the coupon was characterized by measuring the range of pressure differential and air velocity for each angle of treatment (Table 7). The handheld unit used in this experimentation is expected to have less vacuum power when compared to a typical commercial unit. For comparison, the maximum pressure differential and air velocity supplied by a mobile 8 gallon wet/dry vacuum unit at a nozzle angle of 90 degrees were 202 Pa and 17.9 m/s respectively.

Table 7: Measured pressure and air velocity ranges (minimum and maximum values) from handheld vacuum unit at different nozzle angles

Nozzle angle (°)	Pressure (Pa)	Air velocity (m/s)
0	11 – 19	2.5 – 5.4
45	7 – 18	4.3 – 5.5
90	43 – 83	10.7 – 15.3

The efficacy of vacuum-cleaning treatments was assessed by establishing baselines for ATP detection labeled as “clean” and “dirty.” Clean baselines involved swabbing surfaces after cleaning, as outlined in the methodology. For dirty baselines, coupons were swabbed after being coated with either charged or control flour particles. While there was no significant difference in ATP levels between coupons coated with charged or uncharged particles, the clean coupons showed significantly lower readings (Table 8). Based on the results, a mean ATP residue value of 10 RLU was determined as a reasonable cut-off threshold to define “clean” surfaces.

Table 8: ATP swabbed from clean and flour coated stainless steel coupons

	Mean ATP Residues (RLU)
Coupons	Mean ± SD
Charged	138.72 ± 26.44
Control	147.06 ± 34.95
Clean	6.22 ± 2.73

For coupons subjected to the vacuum-cleaning treatment, data were sliced along particle size distributions and relative humidity for analysis. For flour within the 60 – 80 mesh particle distribution, no significant difference was detected between charged and control flour samples at any relative humidity and angle combination. For charged particles at 20% and 40% RH no significant difference was found in ATP level for different angles of application. However, for charged particles at 60% RH, surfaces cleaned with a nozzle angle of 90 degrees had significantly lower ATP level than those cleaned at 0 degrees (*p* value=0.031) (Figure 26).

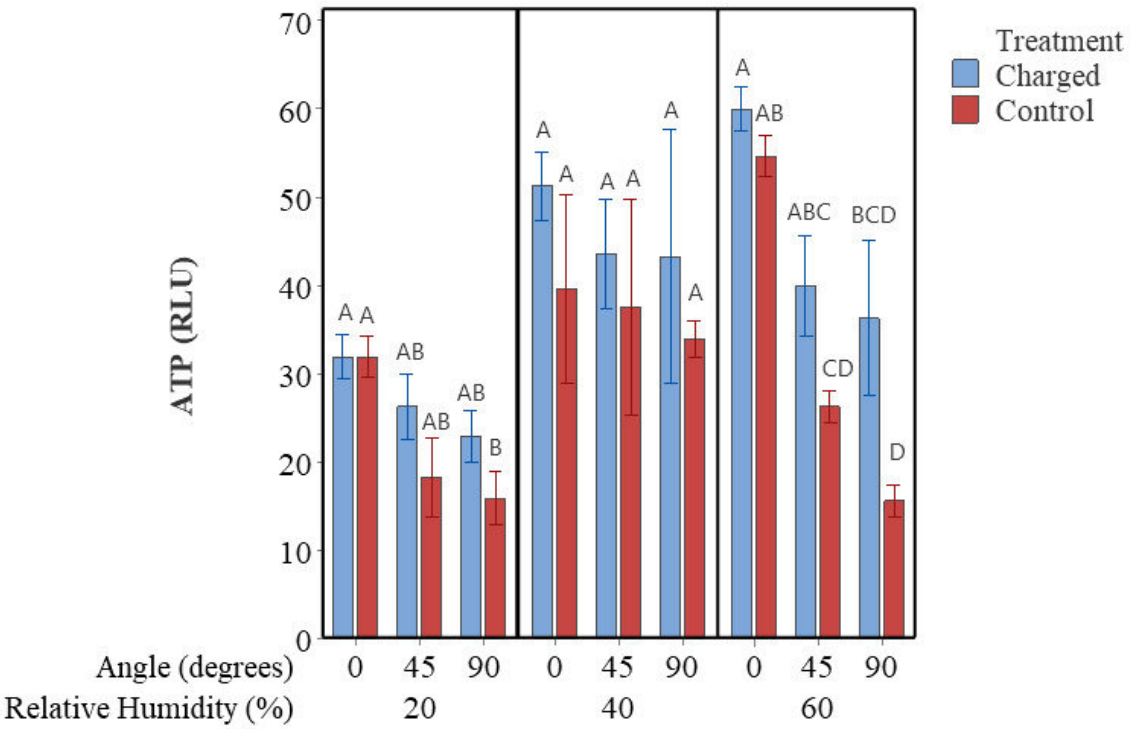

Figure 26: Comparison of ATP residues by relative humidity and angle of vacuum treatment application for 60 – 80 mesh wheat flour. Error bars are one standard error from the mean. Within a panel, means sharing a common letter are not significantly different

For coupons subjected to the vacuum-cleaning treatment, data were sliced along particle size distributions and relative humidity for analysis. Within the 80 – 100 mesh particle size range, there was no significant difference between charged and control flour samples at any relative humidity and angle combination. At 20% and 40% RH, charged particles exhibited no

significant differences in ATP level for different angles of application. However, at 60% RH, surfaces cleaned with a nozzle angle of 90-degree showed significantly lower ATP level compared to a 0-degree angle (*p* value=0.043) (Figure 27).

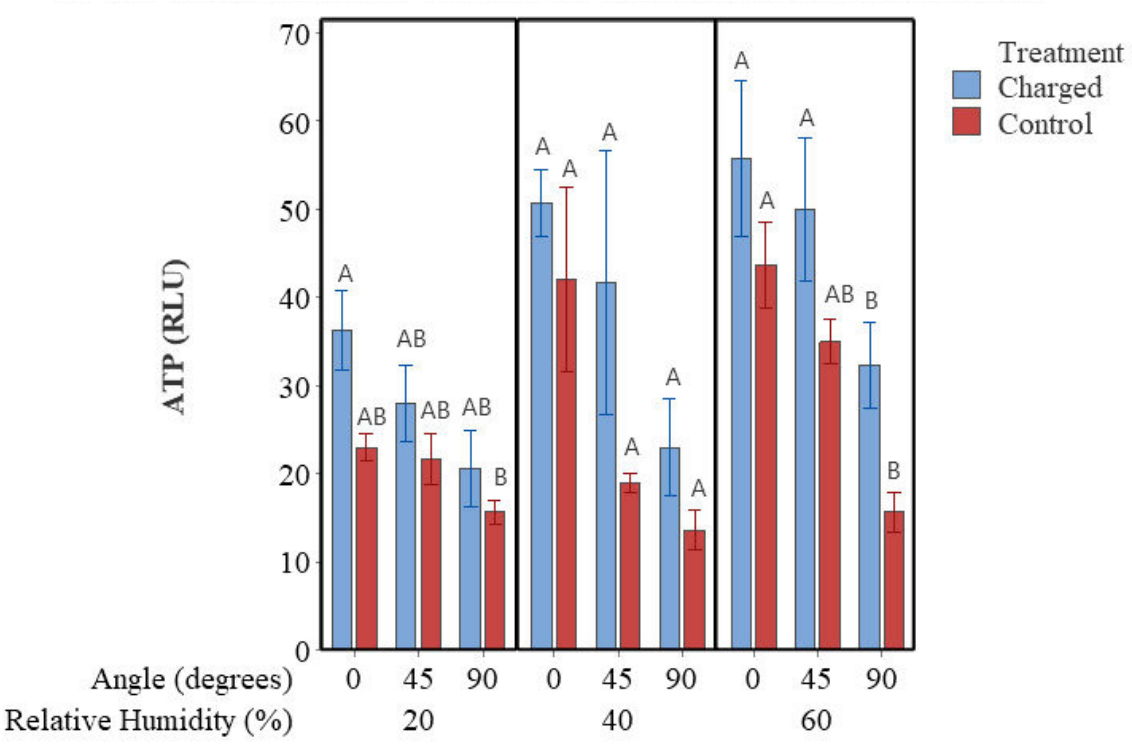

Figure 27: Comparison of ATP residues by relative humidity and angle of vacuum treatment application for 80 – 100 mesh wheat flour. Error bars are one standard error from the mean. Within a panel, means sharing a common letter are not significantly different

When analyzed without slicing of the data, relative humidity emerged as a statistically significant factor (*p* value=0.017). Conversely, particle size and all its interactions did not show any statistical significance. Notably, average ATP levels were observed to increase with rising relative humidity values.

Theoretical Calculations

The theoretical forces of adhesion were calculated using experimentally measured values of charge (Table 3). Due to the low-moisture environment, total adhesion force was considered a combination of electrostatic and Van der Waals forces while capillary forces were assumed to be

negligible. For the calculated adhesion forces, when distance between particle and the surface was assumed to be 5 x 10^{-8} m, electrostatic forces were found to be dominant except in the uncharged control calculations where Van der Waal forces were dominant. The total adhesion force increases exponentially as particle diameter increases because a larger particle can hold more charge.

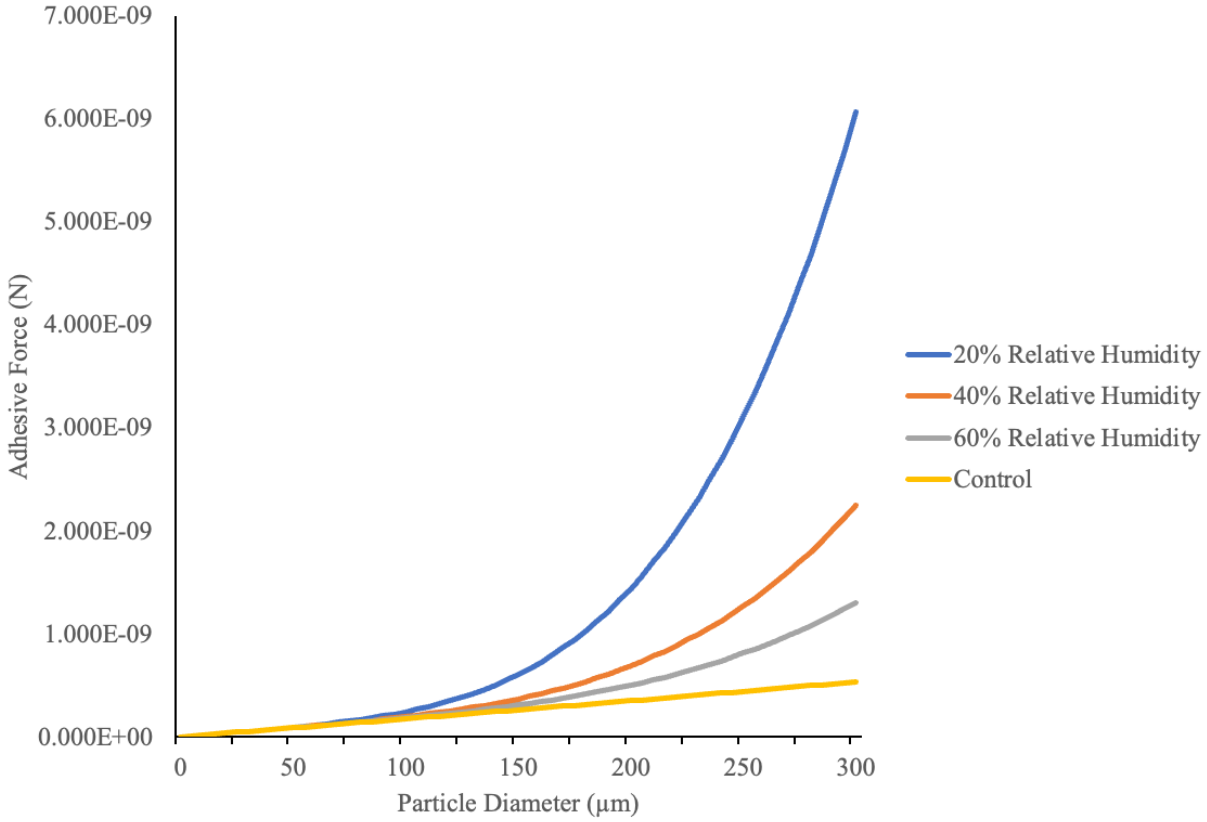

Figure 28: Calculated total adhesion force (h= x 10^{-8} m) for charged and uncharged flour particles on a flat surface based on theoretical equations for Van der Waal and electrostatic forces. Measured charge-to-mass ratios in flour at different relative humidity values were used in electrostatic force calculations

The theoretical IAT removal forces were also calculated using experimentally measured values of deceleration (Table 5). Total force of removal was a combination of the force of the impact and gravitational force. The impact force was more dominant than gravitational force for all tested drop heights. The total removal force increases exponentially as particle diameter

increases due to the increasing mass. The calculated theoretical removal forces were considerably larger than the adhesion forces for all particle diameters when the distance between particle and surface were assumed to be on the larger end of the spectrum, 5 x 10^{-8} m. However, if that distance is shrunk to 5 x 10^{-10} m, the adhesion and removal force graphs more closely match. When distance is diminished, adhesion forces are vastly dominated by van der Waals forces and the impact of electrostatic charge is negligible. This disagrees with our measured practical results that found the factor of treatment (charged or uncharged) to be statistically significant for all tests.

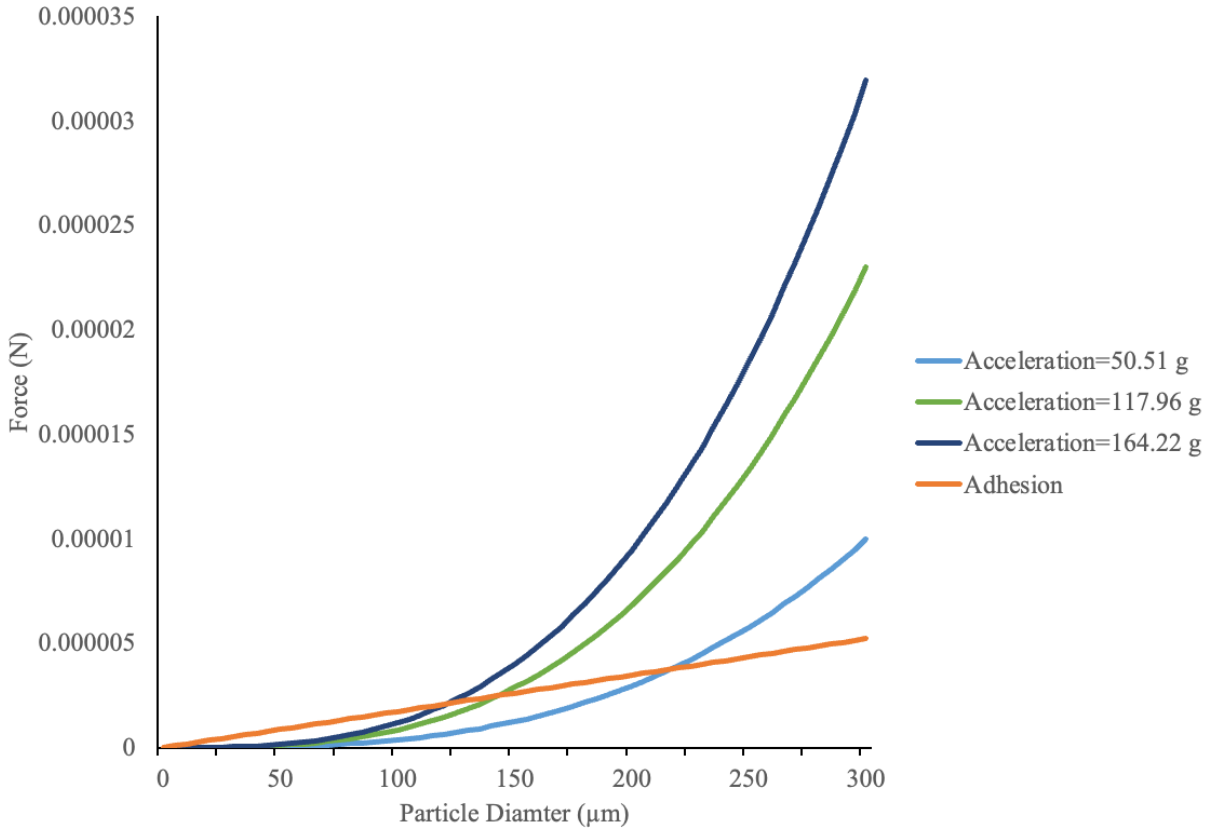

Figure 29: Calculated total removal force and adhesion force (h=5 x 10^{-10} m) for charged and uncharged flour particles on a flat surface based on theoretical equations for gravity and impact forces. Measured deceleration values from impact adhesion tester were used in impact force calculations

Discussion

Relative humidity was found to be a significant factor for vacuum-cleaning, with ATP level generally higher at increased relative humidity levels. The added moisture in the environment at higher relative humidity levels may be increasing the adhesive forces of the flour residues on the coupon surface. The impact of the angle of vacuum nozzle was negligible at 20% and 40% RH. However, at 60% RH, applying vacuum treatments at 90 degrees to the surface resulted in significantly reduced ATP residues compared to 0 degrees application. This implies that in drier conditions (20%, 40% RH), angle of nozzle does not play a significant role. However, in more humid environment (60% RH), a perpendicular vacuum nozzle is more effective in cleaning.

The general trends shown by the calculated theoretical adhesion and removal forces agreed with the measured practical results, while the precise predicted force values did not. The theoretical adhesion equations predicted that as particle diameters decrease, the differences in adhesion force between flour particles of varying charge would lessen. For larger particles there was a greater difference in adhesion forces between flour particles of varying charge. For example, the maximum difference in adhesive force between an uncharged and charged 100 mesh flour particle (149 um diameter) was predicted to be 3.45×10^{-10} N. Whereas, the maximum difference in adhesive force between an uncharged and charged 60 mesh particle (250 um diameter) was predicted to be 2.67×10^{-9} N. Therefore, the difference in predicted adhesion forces between charged and uncharged particles is 7.72 times greater for 60 mesh particles over 100 mesh particles. This agrees with the measured results where charged flour within the larger (60 – 80 mesh) particle range displayed significantly higher flour retention than uncharged flour.

Flour within the smaller (80 – 100 mesh) particle range did not show a difference in flour retention between charged and uncharged samples.

The theoretically calculated removal forces were greater than the adhesion forces for all particle diameters. This implies that 100% of the adhered flour should have been removed for any of the impact adhesion tests. However, these results disagree with the practical results, which had retention rates as high as 60%. The reason for this difference can be attributed to the assumptions necessary to use the theoretical equations. Theoretical equations assume perfectly spherical particle shape and smooth surfaces. Most importantly, the assumption made for distance between particle surface and stainless steel surface, h, can drastically impact the theoretical Van der Waals forces. This is because as the distance approaches 0, the van Der Waals forces go to infinity. Therefore, previous studies quantifying starch particle adhesion to stainless steel surfaces have used or predicted values ranging from 5×10^{-8} m (Ermis et al., 2011; Huang & Barringer, 2012) to 5×10^{-10} m (Salazar-Banda et al., 2007).

This highlights the limitations in using theoretical equations as predictors for particle adhesion in real-life situation and the necessity of using empirical results to assist decisions. Although theoretical particle adhesion equations can be a useful tool for predicting trends, estimating precise force values is very challenging.

CONCLUSIONS

The study set out with three clearly defined objectives and through systematic experimentation and analysis, these goals were successfully accomplished. This section provides a synthesis of the findings, elucidates the relevance of the outcomes to the area of study, and suggests future work as follows:

Objective 1: Simulating and Measuring Triboelectric Charge Generation in Flour

- The use of a short (61 cm) stainless steel tube for triboelectric charging of flour samples proved to be an effective, simple, and cost-effective methodology. Flour samples exhibited a significantly higher charge than control samples after undergoing the charging tube treatment, regardless of relative humidity. Furthermore, the amount of charge achieved by flour samples remained relatively consistent within each relative humidity, with the largest standard deviation being under 1 nC/g.
- The importance of relative humidity on tribocharging was highlighted. Flour samples charged at 20% relative humidity exhibited significantly higher charge values compared to those charged at 40% or 60%, indicating that drier conditions might be more prone to issues related to the triboelectric charging of powders.
- Particle size showed no significant impact on triboelectrification across the particle sizes. Flour within both the 60 – 80 mesh and 80 – 100 mesh range showed comparable charge-to-mass ratio (nC/g) for each treatment conditions. However, due to the greater mass of larger particles, more charge is held in an individual 60 – 80 mesh particle when compared to an individual 80 – 100 mesh particle, a distinction that is reflected in the adhesion test results.

Objective 2: Quantifying Adhesion of Flour on Stainless Steel Surfaces

- The impact adhesion tester was successfully able to generate consistent deceleration values for a given drop height. Using the IAT, the influence of charge, relative humidity and size on adhesion rate trends were established. However, with the current equipment, 100% of flour particle removal from the stainless steel coupons was not achievable. This made it difficult to fully characterize the adhesion of particles within a given size range and to determine the minimum amount of force necessary to remove all particles.
- Charged flour within the larger (60 – 80 mesh) particle range displayed significantly higher flour retention than uncharged flour. Flour within the smaller (80 – 100 mesh) particle range did not show a difference in flour retention between charged and uncharged samples. This indicates that sufficiently fine flour (>80 mesh) is less prone to increased adhesion due to triboelectric charging.
- Charged flour within the larger (60 – 80 mesh) particle range exhibited significantly higher retention rates for tests performed at 20% relative humidity when compared to those at 60%. This agrees with the chargeability tests that found that electrostatic charge was greater at 20% relative humidity. This suggests that the increase in particle retention at 20% relative humidity can be primarily attributed to the effects of electrostatic charge.
- Larger flour particles (60 – 80 mesh) trended to have higher adhesion rates than smaller flour particles (80 – 100 mesh). This agrees with the findings of previous research (Mayr & Barringer, 2006; Salazar-Banda et al., 2007) into adhesion of food particles, and can be partially explained by larger particles being able to hold greater electrostatic charge.

Objective 3: Factors Impacting the Efficacy of Vacuum Cleaning

- Due to the limited space within the humidity-controlled chambers, a small handheld vacuum was used for testing rather than a larger equipment more representative of industry practice. Despite this limitation, the small vacuum unit was still able to clean coupons to a level where no particles could be identified visually, and there was no detectable difference in mass from a "clean" coupon. This level of clean was achieved for any combination of charge, relative humidity, and particle size. This implies that typical industrial vacuums would be fully capable of supplying enough force to remove visible flour particles adhered by only Van der Waals and electrostatic forces.
- Despite all coupons being cleaned to a level of "visually clean", ATP residues from flour could still be detected at levels greater than 10 RLU for all treatments. This agrees with the findings published by Jackson et al. (2008), where ELISA, protein swabs, and ATP swabs were still able to detect residues after vacuuming removed the loosely adhered particles. These results suggest that while vacuuming alone can remove most visible flour particles, trace residues can remain that may require an additional cleaning step.
- Relative humidity was found to be a significant factor for vacuum-cleaning, with ATP residues generally higher at increased relative humidity levels. The increased moisture present at higher relative humidity levels may enhance the adhesive properties of the flour residues on the coupon surface. Since vacuum cleaning proved effective in removing visible flour particles at lower relative humidity levels (20%), despite the observed increase in adhesion, it is advisable for food manufacturing facilities to maintain a lower relative humidity to minimize the presence of more hard-to-clean flour residues.

- The vacuum nozzle angle had negligible impact at 20% and 40% RH. However, at 60% RH, using the vacuum at a 90-degree angle to the surface significantly reduced ATP residues compared to an application at 0 degrees. This implies that in drier conditions (20%, 40% RH), the nozzle angle is less critical. In contrast, in a more humid environment (60% RH), a perpendicular vacuum nozzle orientation enhances cleaning effectiveness.

Future Work

A broader goal of the Food Safety and Modernization Act was to protect the public health by researching and implementing scientifically backed preventative controls. This mission does not only apply to safety hazards within food manufacturing facilities, but to hazards throughout the entire food production process, from farm to fork. This research certainly contributes to the body of knowledge surrounding cleaning in low-moisture environments; however, there exists many other avenues in which the efficacy of dry-cleaning methodologies can be explored.

The research presented in this thesis attempted to simulate the triboelectrification and adhesion of wheat flour in contact with stainless steel during processing within a plant. While the general trends presented in the research can be applicable to other food safety scenarios, it is desirable to research additional combinations of materials and factors. Future work could investigate the impact of other common surfaces found within a food production facility (stainless steel, teflon, polyethylene, urethane, and polycarbonate) on triboelectrification and adhesion. The factor of surface roughness and finish on stainless steel adhesion should also be investigated. Additionally, other particulates common to low-moisture food production should be investigated. This could be other low-moisture food powders (milk powder, sugars, or starches or spices) or non-food debris, such as dust and dirt accumulation during harvesting.

While the charging method was effective, future work could take measures to further standardize application of charge to powders. Rather than manually shaking the tube to promote powder flow, a vibratory feeder could be developed. Additionally, charging tubes made of different materials could be developed to investigate which surfaces promote static charge build-up more effectively.

The sieve shaker was able to loosely characterize flour particles within a range of mesh sizes. For future work more could be done to analyze the size and shape distributions of flour particles. Microscopy could be performed to visualize the particles and their distribution across a coupon surface. Alternatively, a particle size analyzer, such as a Malvern Mastersizer, could be used to characterize the flour particles.

The strength of the handheld vacuum cleaner was characterized by measuring the range of airspeed and pressure differential at the surface of a coupon. While these parameters can be useful for understanding the strength of a vacuum cleaner, it is difficult to calculate the precise removal force, and doing so was beyond the scope of this research. Future work could attempt to model and simulate the combined impact of airflow and suction power on the removal of particles on a surface. Calculating the minimum combination of airflow and suction required to remove a particle would be a useful parameter for industrial decision-making.

The results of the theoretical calculations highlighted the challenges of using fundamental equations for predicting precise adhesion values. The number of assumptions required to apply these equations frequently lead to predictions that are not accurately aligned with the measured results. Therefore, the development of an empirical model to predict particle adhesion would be highly beneficial for the industry. This model would allow for the input of specific particle and

surface characteristics, outputting the minimum force necessary for particle removal. Such a tool could greatly assist in industrial decision-making processes.

BIBLIOGRAPHY

Acuff, J. C., Dickson, J. S., Farber, J. M., Grasso-Kelley, E. M., Hedberg, C., Lee, A., & Zhu, M.-J. (2023). Practice and progress: Updates on outbreaks, advances in research, and processing technologies for low-moisture food safety. *Journal of Food Protection*, *86*(1), Article 100018. https://doi.org/10.1016/j.jfp.2022.11.010

Aremu, D., Babajide, N., & Ogunlade, C. (2014). Comparison of some engineering properties of common cereal grains in Nigeria. *International Journal of Engineering Science Invention*, *3*(4).

Bailey, A. G. (1984). Electrostatic phenomena during powder handling. *Powder Technology*, *37*(JAN-), 71-85. https://doi.org/10.1016/0032-5910(84)80007-8

Bakerpedia. (2020). *All-purpose flour*. https://bakerpedia.com/ingredients/all-purpose-flour/

Benoit, A. N. (2013). *Experimental and mathematical models for Listeria monocytogenes transfer between delicatessen meats and contact surfaces* [Masters thesis, Michigan State University]. ProQuest.

Butt, H.-J. (2008). Capillary forces: Influence of roughness and heterogeneity. *Langmuir*, *24*(9), 4715-4721. https://doi.org/10.1021/la703640f

Centers for Disease Control and Prevention, Division of Foodborne, Waterborne, and Environmental Diseases (DFWED) (2021). *E. coli outbreak linked to cake mix*. https://www.cdc.gov/ecoli/2021/o121-07-21/index.html

Chen, L., Rana, Y. S., Heldman, D. R., & Snyder, A. B. (2022). Environment, food residue, and dry cleaning tool all influence the removal of food powders and allergenic residues from stainless steel surfaces. *Innovative Food Science & Emerging Technologies*, *75*, Article 102877. https://doi.org/10.1016/j.ifset.2021.102877

Chen, L., & Snyder, A. B. (2023). Surface inoculation method impacts microbial reduction and transfer of *Salmonella* Enteritidis PT 30 and potential surrogates during dry sanitation. *International journal of food microbiology*, *406*, 110405-110405. https://doi.org/10.1016/j.ijfoodmicro.2023.110405

Cheng, W., Dunn, P. F., & Brach, R. M. (2002). Surface roughness effects onmicroparticle adhesion. *Journal of Adhesion*, *78*(11), 929-965. https://doi.org/10.1080/00218460214510

Chowdhury, F., Ray, M., Sowinski, A., Mehrani, P., & Passalacqua, A. (2021). A review on modeling approaches for the electrostatic charging of particles. *Powder Technology*, *389*, 104-118. https://doi.org/10.1016/j.powtec.2021.05.016

Crowe, S. J., Bottichio, L., Shade, L. N., Whitney, B. M., Corral, N., Melius, B., Arends, K. D., Donovan, D., Stone, J., Allen, K., Rosner, J., Beal, J., Whitlock, L., Blackstock, A., Wetherington, J., Newberry, L. A., Schroeder, M. N., Wagner, D., Trees, E., Viazis, S.,

… Neil, K. P. (2017). Shiga Toxin-Producing E. coli Infections Associated with Flour. *The New England journal of medicine*, *377*(21), 2036–2043. https://doi.org/10.1056/NEJMoa1615910

Daeschel, D., Rana, Y. S., Chen, L., Cai, S., Dando, R., & Snyder, A. B. (2023). Visual inspection of surface sanitation: Defining the conditions that enhance the human threshold for detection of food residues. *Food Control*, *149*, Article 109691. https://doi.org/10.1016/j.foodcont.2023.109691

Ermis, E., Farnish, R. J., Berry, R. J., & Bradley, M. S. A. (2011). Centrifugal tester versus a novel design to measure particle adhesion strength and investigation of effect of physical characteristics (size, shape, density) of food particles on food surfaces. *Journal of Food Engineering*, *104*(4), 518-524. https://doi.org/10.1016/j.jfoodeng.2011.01.008

Ermis, E., (2011) *Establishment of a repeatable test procedure for measuring adhesion strength of particulates in contact with surfaces*. [Doctoral dissertation, University of Greenwich]. ProQuest.

Forghani, F., den Bakker, M., Liao, J.-Y., Payton, A. S., Futral, A. N., & Diez-Gonzalez, F. (2019). *Salmonella* and enterohemorrhagic *Escherichia coli* serogroups O45, O121,O145 in wheat flour: Effects of long-term storage and thermal treatments. *Frontiers in Microbiology*, *10*, Article 323. https://doi.org/10.3389/fmicb.2019.00323

Gill, A., McMahon, T., Dussault, F., & Petronella, N. (2020). Shiga toxin-producing *Escherichia coli* survives storage in wheat flour for two years. *Food Microbiology*, *87*, Article 103380. https://doi.org/10.1016/j.fm.2019.103380

Hammons, S. R., Stasiewicz, M. J., Roof, S., & Oliver, H. F. (2015). Aerobic plate counts and ATP levels correlate with Listeria monocytogenes detection in retail delis. *Journal of food protection*, *78*(4), 825–830. https://doi.org/10.4315/0362-028X.JFP-14-500

Huang, Y., & Barringer, S. A. (2012). Adhesion of food powders with nonelectrostatic and electrostatic coating. *Journal of Food Process Engineering*, *35*(2), 264-277. https://doi.org/10.1111/j.1745-4530.2010.00587.x

Jackson, L. S., Al-Taher, F. M., Moorman, M., DeVries, J. W., Tippett, R., Swanson, K. M., Fu, T., Salter, R., Dunaif, G., Estes, S. (2008). Cleaning and other control and validation strategies to prevent allergen cross-contact in food-processing operations. *Journal of Food Protection*, *71*(2), 445-458.

Klug, I.M., Suehr, Q.J., Marks, B.P., Jeong, S. (2022). *Quantifying the electrostatic adhesion force of powders on food contact surfaces for dry cleaning and sanitation.* Poster session presentation at the meeting of the International Association for Food Protection, Pittsburgh, PA.

Kohli, R., & Mittal, K. L. (2019). Methods for assessing surface cleanliness. In R. Kohli & K. L. Mittal (Eds.), *Developments in surface contamination and cleaning, Vol 12: Methods for*

assessment and verification of cleanliness of surfaces and characterization of surface contaminants (pp. 23-105). https://doi.org/10.1016/b978-0-12-816081-7.00003-6

Lauer, J. R., Simsek, S., & Bergholz, T. M. (2021). Fate of *Salmonella* and enterohemorrhagic *Escherichia coli* on wheat grain. *Journal of Food Protection*, *84*(12), 2109-2115. https://doi.org/10.4315/jfp-21-076

Matsusaka, S., Maruyama, H., Matsuyama, T., & Ghadiri, M. (2010). Triboelectric charging of powders: A review. *Chemical Engineering Science*, *65*(22), 5781-5807. https://doi.org/10.1016/j.ces.2010.07.005

Mayr, M. B., & Barringer, S. A. (2006). Corona compared with triboelectric charging for electrostatic powder coating. *Journal of Food Science*, *71*(4), E171-E177. https://doi.org/10.1111/j.1750-3841.2006.00024.x

Moerman, F., & Mager, K., (2016). Cleaning and disinifection in dry food processing facilities. In H. Lelieveld, J. Holah, & D. Gabric (Eds.), *Handbook of hygiene control in the food industry. Second edition* (Chapter 35). Woodhead Publishing.

Myoda, S. P., Gilbreth, S., Akins-Leventhal, D., Davidson, S. K., & Samadpour, M. (2019). Occurrence and levels of *Salmonella*, enterohemorrhagic *Escherichia coli*, and *Listeria* in raw wheat. *Journal of Food Protection*, *82*(6), 1022-1027. https://doi.org/10.4315/0362-028x.jfp-18-345

Peltonen, J. (2019). *Electrostatic instrumentation and measurements on powders and powder mixtures*. [Doctoral dissertation, University of Turku]. ProQuest

Peltonen, J., Murtomaa, M., & Salonen, J. (2018). Measuring electrostatic charging of powders on-line during surface adhesion. *Journal of Electrostatics*, *93*, 53-57. https://doi.org/10.1016/j.elstat.2018.03.007

Podolak, R., Enache, E., Stone, W., Black, D. G., & Elliott, P. H. (2010). Sources and risk factors for contamination, survival, persistence, and heat resistance of *Salmonella* in low-moisture foods [Review]. *Journal of Food Protection*, *73*(10), 1919-1936. https://doi.org/10.4315/0362-028x-73.10.1919

Quanrun, H., Long, C., & Abigail, B. S. (2022). The physicochemical properties of fruit powders and their residence time on stainless steel surfaces are associated with their ease of removal by brushing. *Food Research International*, *158*, 111569-111569. https://doi.org/10.1016/j.foodres.2022.111569

Rabinovich, Y. I., Adler, J. J., Esayanur, M. S., Ata, A., Singh, R. K., & Moudgil, B. M. (2002). Capillary forces between surfaces with nanoscale roughness [Article]. *Advances in colloid and interface science*, *96*(1-3), 213-230, Article Pii s0001-8686(01)00082-3. https://doi.org/10.1016/s0001-8686(01)00082-3

Ricks, N. P., Barringer, S. A., & Fitzpatrick, J. J. (2002). Food powder characteristics important to nonelectrostatic and electrostatic coating and dustiness. *Journal of Food Science*, *67*(6), 2256-2263. https://doi.org/10.1111/j.1365-2621.2002.tb09537.x

Salazar-Banda, G. R., Felicetti, M. A., Goncalves, J. A. S., Coury, J. R., & Aguiar, M. L. (2007). Determination of the adhesion force between particles and a flat surface, using the centrifuge technique [Article]. *Powder Technology*, *173*(2), 107-117. https://doi.org/10.1016/j.powtec.2006.12.011

Smith, D. F., & Marks, B. P. (2015). Effect of rapid product desiccation or hydration on thermal resistance of Salmonella enterica serovar Enteritidis PT 30 in wheat flour. *Journal of Food Protection*, *78*(2), 281-286.

Sogin, J. H., Lopez Velasco, G., Yordem, B., Lingle, C. K., David, J. M., Cobo, M., & Worobo, R. W. (2021). Implementation of ATP and Microbial Indicator Testing for Hygiene Monitoring in a Tofu Production Facility Improves Product Quality and Hygienic Conditions of Food Contact Surfaces: A Case Study. *Applied and environmental microbiology*, *87*(5), e02278-20. https://doi.org/10.1128/AEM.02278-20

Stotzel, H., Schmidt, H. J., Auerbach, D., Makin, B., Dastoori, K., & Bauch, H. (1997). Adhesion measurements for electrostatic powder coatings. *Journal of Electrostatics*, *40-1*, 253-258. https://doi.org/10.1016/s0304-3886(97)00046-6

Suehr, Q. J. (2020). *Adhesion mechanics and physical characteristics of Salmonella enteritidis in low moisture environments* [Masters thesis, Michigan State University]. ProQuest.

Taylor, S. L., S. L. Hefle, A. K. Farnum, S. W. Rizk, J. Yeung, M. E. Barnett, F. Busta, F. R. Shank, R. Newsome, S. Davis, and C. Bryant. (2006). Analysis and evaluation of food manufacturing practices used to address allergen concerns. *Comprehensive Reviews in Food Science and Food Safety* 5:138–157. https://doi-org.proxy1.cl.msu.edu/10.1111/j.1541-4337.2006.00012.x

Title 21, 2 C.F.R. § 137.105 (1977). https://www.accessdata.fda.gov/scripts/cdrh/cfdocs/cfcfr/CFRSearch.cfm?fr=137.105

United States Food and Drug Administration (2019). *Recall of glass jars of in the mix, Brand Castle and Sisters' Gourmet Baking Mixes because of possible health risk.* https://www.fda.gov/safety/recalls-market-withdrawals-safety-alerts/recall-glass-jars-mix-brand-castle-and-sisters-gourmet-baking-mixes-because-possible-health-risk#:~:text=The%20product%20is%20being%20recalled,at%20their%20Buffalo%20production%20plant

United States Food and Drug Administration (2023). *Outbreak investigation of Salmonella: flour.* https://www.fda.gov/food/outbreaks-foodborne-illness/outbreak-investigation-salmonella-flour-april-2023#:~:text=The%20FDA%2C%20along%20with%20CDC,that%20the%20outbreak%20is%20over.

World Health Organization. (1995). Surveillance programme. *Sixth report of WHO surveillance program for control of foodborne infections and intoxications in Europe. FAO/WHO Collaborating Centre for Research and Training in food Hygiene and Zoonoses, Berlin*.

You, S., & Wan, M. P. (2013). Mathematical models for the van der Waals force and capillary force between a rough particle and surface [Article]. *Langmuir*, *29*(29), 9104-9117. https://doi.org/10.1021/la401516m

You, S., & Wan, M. P. (2014). Modeling and experiments of the adhesion force distribution between particles and a surface [Article]. *Langmuir*, *30*(23), 6808-6818. https://doi.org/10.1021/la500360f

APPENDIX

All pairwise comparisons were conducted using Minitab statistical software. Grouping was conducted using the Tukey method with 95% confidence intervals. Means sharing a common letter are not significantly different.

Table 9: Mean values and grouping for chargeability tests

Grouping Information Using the Tukey Method and 95% Confidence						
Relative humidity (%)* Mesh size* Treatment	N	Mean	Grouping			
20 60 Charged	3	6.06060	A			
20 80 Charged	3	5.89253	A			
40 80 Charged	3	3.42739		B		
40 60 Charged	3	3.25115		B		
60 60 Charged	3	2.47564		B		
60 80 Charged	3	2.01701		B	C	
40 80 Control	3	0.48354			C	D
20 80 Control	3	0.40457			C	D
40 60 Control	3	0.30185				D
20 60 Control	3	0.30110				D
60 60 Control	3	0.17543				D
60 80 Control	3	0.14928				D

Table 10: Mean values and grouping for adhesion tests

Relative humidity(%)* Mesh size* Treatment* Drop height(in)	N	Mean	Grouping								
20 60 Charged 1	3	59.3742	A								
40 60 Charged 1	3	53.7869	A	B							
20 60 Charged 5	3	48.1814	A	B	C						
20 80 Charged 1	3	46.9860	A	B	C	D					
60 80 Uncharged 1	3	46.3559	A	B	C	D					
60 80 Charged 1	3	45.9682	A	B	C	D					
40 80 Charged 1	3	42.5216	A	B	C	D	E				
20 80 Uncharged 1	3	42.3201	A	B	C	D	E				
20 80 Charged 5	3	41.0523	A	B	C	D	E	F			
20 60 Charged 9	3	38.6111		B	C	D	E	F	G		
60 60 Charged 1	3	36.5336		B	C	D	E	F	G	H	
40 60 Charged 5	3	36.4308		B	C	D	E	F	G	H	
20 60 Uncharged 1	3	32.4990			C	D	E	F	G	H	I
20 80 Uncharged 5	3	30.0543			C	D	E	F	G	H	I	J
20 80 Charged 9	3	29.5758				D	E	F	G	H	I	J
40 80 Uncharged 1	3	28.9442				D	E	F	G	H	I	J
60 60 Uncharged 1	3	28.7325				D	E	F	G	H	I	J
20 60 Uncharged 5	3	25.8665					E	F	G	H	I	J
60 60 Charged 5	3	25.5926					E	F	G	H	I	J
40 60 Charged 9	3	25.5579					E	F	G	H	I	J
40 60 Uncharged 1	3	24.2609					E	F	G	H	I	J
60 80 Charged 5	3	23.0484						F	G	H	I	J
60 60 Uncharged 5	3	23.0159						F	G	H	I	J
20 60 Uncharged 9	3	22.0572							G	H	I	J
40 80 Charged 5	3	22.0134							G	H	I	J
60 80 Uncharged 5	3	20.1329								H	I	J
40 80 Uncharged 5	3	19.9267								H	I	J
60 60 Charged 9	3	18.6667								H	I	J
40 80 Charged 9	3	18.3778								H	I	J
20 80 Uncharged 9	3	17.5559									I	J
40 60 Uncharged 5	3	15.7645									I	J
60 60 Uncharged 9	3	15.5678									I	J
60 80 Charged 9	3	15.0344									I	J
40 80 Uncharged 9	3	14.4468									I	J
40 60 Uncharged 9	3	13.4135										J
60 80 Uncharged 9	3	13.1216										J

Table 11: Mean values and grouping for vacuum cleanability tests

Relative humidity(%)* Mesh size* Treatment* Angle	N	Mean	Grouping						
60 60 Charged 0	3	60.0000	A						
60 80 Charged 0	3	55.6667	A	B					
60 60 Uncharged 0	3	54.6667	A	B	C				
40 60 Charged 0	3	51.3333	A	B	C	D			
40 80 Charged 0	3	50.6667	A	B	C	D	E		
60 80 Charged 45	3	50.0000	A	B	C	D	E	F	
40 60 Charged 45	3	43.6667	A	B	C	D	E	F	G
60 80 Uncharged 0	3	43.6667	A	B	C	D	E	F	G
40 60 Charged 90	3	43.3333	A	B	C	D	E	F	G
40 80 Uncharged 0	3	42.0000	A	B	C	D	E	F	G
40 80 Charged 45	3	41.6667	A	B	C	D	E	F	G
60 60 Charged 90	3	40.0000	A	B	C	D	E	F	G
40 60 Uncharged 0	3	39.6667	A	B	C	D	E	F	G
40 60 Uncharged 45	3	37.6667	A	B	C	D	E	F	G
20 80 Charged 0	3	36.3333	A	B	C	D	E	F	G
60 60 Charged 45	3	36.3333	A	B	C	D	E	F	G
60 80 Uncharged 45	3	35.0000	A	B	C	D	E	F	G
40 60 Uncharged 90	3	34.0000	A	B	C	D	E	F	G
60 80 Charged 90	3	32.3333	A	B	C	D	E	F	G
20 60 Charged 0	3	32.0000	A	B	C	D	E	F	G
20 60 Uncharged 0	3	32.0000	A	B	C	D	E	F	G
20 80 Charged 45	3	28.0000	A	B	C	D	E	F	G
20 60 Charged 45	3	26.3333	A	B	C	D	E	F	G
60 60 Uncharged 45	3	26.3333	A	B	C	D	E	F	G
20 80 Uncharged 0	3	23.0000		B	C	D	E	F	G
40 80 Charged 90	3	23.0000		B	C	D	E	F	G
20 60 Charged 90	3	23.0000		B	C	D	E	F	G
20 80 Uncharged 45	3	21.6667		B	C	D	E	F	G
20 80 Charged 90	3	20.6667			C	D	E	F	G
40 80 Uncharged 45	3	19.0000				D	E	F	G
20 60 Uncharged 45	3	18.3333				D	E	F	G
20 60 Uncharged 90	3	16.0000					E	F	G
20 80 Uncharged 90	3	15.6667						F	G
60 80 Uncharged 90	3	15.6667						F	G
60 60 Uncharged 90	3	15.6667						F	G
40 80 Uncharged 90	3	13.6667							G